NRC Research Press

ARTICLE

Microsedimentological evidence of vertical fluctuations in subglacial stress from the northwest sector of the Laurentide Ice Sheet, Northwest Territories, Canada

Jessey M. Rice, John Menzies, Roger C. Paulen, and M. Beth McClenaghan

Abstract: The past-producing Pine Point lead–zinc mining district, Northwest Territories, Canada, provides a unique opportunity to study the role of glacial dynamics in a thick, continuous till succession that has not been influenced by the underlying bedrock topography. Parts of the Pine Point mining district are covered by >20 m of subglacial Quaternary sediments (till) associated with the former Laurentide Ice Sheet. Till facies exposed in unreclaimed open-pit K-62 have been classified into four separate units. Micro- and macrosedimentological analyses were undertaken to identify the change in subglacial stress during sediment deposition and across till unit boundaries. An analysis of high- and low-angle microshears (lineations) in thin sections produced from these till units indicate that there is a noticeable decrease in the abundance of low-angle shear features immediately below till unit boundaries. The deformation of low-angle shears in the underlying tills was likely caused by remobilization of the overlying till unit. This remobilization is consistent with aggradation-constant entrainment decay mechanisms for subglacial till emplacement and accretion and subglacial dispersion models.

Résumé : Le district minier de Pine Point, ancien producteur de plomb et zinc dans les Territoires-du-Nord-Ouest (Canada), offre une occasion unique d'étudier le rôle de la dynamique des glaces dans une séquence épaisse et continue de till n'ayant pas été influencée par le relief de substrat rocheux sous-jacent. Des secteurs du district minier de Pine Point sont recouverts de >20 m de sédiments quaternaires sous-glaciaires (till) associés à l'ancien inlandsis laurentidien. Des faciès de till exposés dans la fosse non restaurée K-62 ont été classés dans quatre unités distinctes. Des analyses micro- et macrosédimentologiques ont été réalisées afin de cerner les variations des contraintes sous-glaciaires durant le dépôt de sédiments et entre les unités de till. Une analyse de microcisaillements (linéations) fortement et faiblement inclinés en lames minces dans ces unités de till indique une diminution perceptible de l'abondance des éléments de cisaillement faiblement inclinés immédiatement sous les limites d'unités de till. La déformation des cisaillements faiblement inclinés dans des tills sous-jacents est probablement le résultat de la mobilisation des unités de till sus-jacentes. Cette mobilisation concorde avec des mécanismes d'alluvionnement-décomposition par entraînement constant pour la mise en place/l'accrétion sous-glaciaires de tills et des modèles de dispersion sous-glaciaire.

Introduction

The role of subglacial sediments in the movement of continental ice sheets is important but not entirely understood (Benn and Evans 1998; Boulton 2006; Evans et al. 2006; Menzies et al. 2018; Evans 2018). A classic approach to understanding how these large ice sheets changed over time has been to separate till into different units based on sedimentological differences between units. However, the type of glacial dynamics that causes the defined till unit separation (i.e., till sub-units) remains largely uncharacterized (cf. Banham 1988; Hart et al. 1990; Roberts and Hart 2005; Lee and Phillips 2008). More specifically, changes in shear stress and how it affects till erosion, deformation, and accretion remains unresolved (cf. Hooyer and Iverson 2000; Larsen et al. 2006*a*; Iverson 2010; Reinardy et al. 2011).

Micromorphology (or more broadly, microsedimentology) involves the microscopic investigation of the structures within undisturbed and often unconsolidated, sediments and aids in the investigation of more traditional macroscopic sediment investigations (Carr 2004). Micromorphology has been used to identify microstructures in seemingly massive till, providing important information on the genesis, deformation, and strain history of the sediments (cf. van der Meer 1993; Phillips et al. 2013; Menzies et al. 2018). The use of micromorphology in the examination of glacial sediments has been successful in discerning subtle differences between macroscopically similar sediments such as debris flows, subglacial tills, glaciomarine sediments, and glaciolacustrine sediments (cf. Licht et al. 1999; Carr 2001; Menzies and Zaniewski 2003). Ultimately, the use of micromorphology in the investigation of glacial sediments has proven to be a powerful tool when used with traditional sedimentological analysis in augmenting our understanding of sediment associations.

Over the last several decades, the use of microsedimentology in the analysis of glacial sediments has considerably advanced the understanding of how subglacial sediments deform and are how they are deposited (cf. van der Meer 1997; Menzies 2000; van der Meer et al. 2003; Larsen et al. 2004, 2006*b*; Menzies et al. 2006; Phillips et al. 2007; Neudorf et al. 2015; Spagnolo et al. 2016). Other

Received 2 August 2018. Accepted 8 November 2018.

Paper handled by Associate Editor Alan Trenhaile.

J.M. Rice. Department of Earth and Environmental Science, University of Waterloo, Waterloo, ON N2L 3G1, Canada.
J. Menzies. Department of Earth Sciences, Brock University, St. Catharines, ON L2S 3A1, Canada.
R.C. Paulen and M.B. McClenaghan. Geological Survey of Canada, Ottawa, ON K1A 0E9, Canada.

Corresponding author: Jessey Rice (email: j4rice@uwaterloo.ca).

Fig. 1. Location of the study area in northern Canada (top left) within the regional context of the Canadian Shield and Western Canadian Sedimentary Basin. Eskers and glacial landforms are taken from The Geological Survey of Canada Surficial Map of Canada (Fulton 1995). Lower right inset: Spot imagery showing the location of open-pit K-62 within the past-producing Pine Point lead–zinc mining district. [Colour online.]

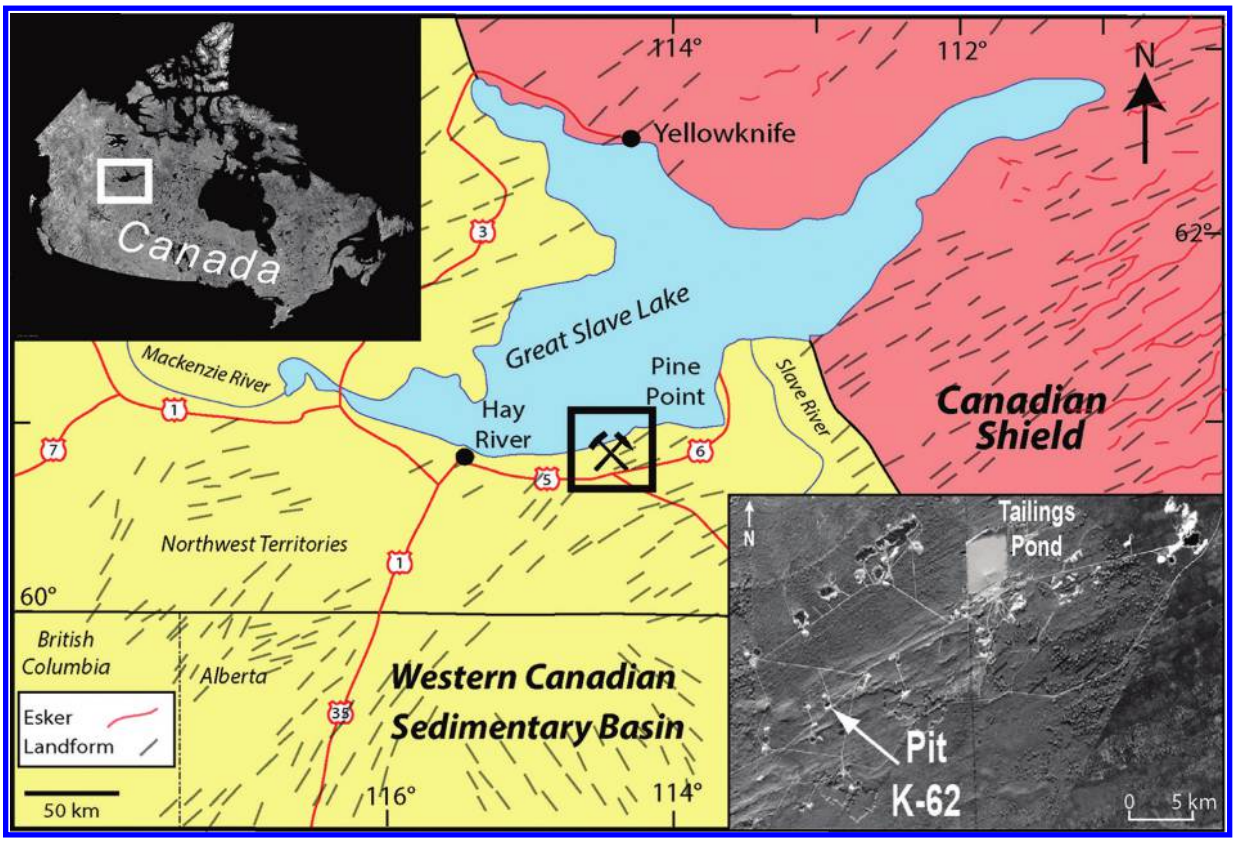

micromorphological studies have focused on defining a variety of glacial sediments (e.g., Phillips and Auton 2000; Lee and Phillips 2008; Phillips and Merritt 2008; Denis et al. 2010; Vaughan-Hirsch et al. 2013), have analyzed comparative samples from multiple sites (e.g., van der Meer 1993; Menzies 2000; Phillips et al. 2007; Neudorf et al. 2013), or have been conducted on glacial sediment samples taken from boreholes (Maltman 1988; Menzies and Maltman 1992; van der Meer 1997; Carr 1998, 1999; Carr et al. 2000; Eyles et al. 2011; Hodder et al. 2016). Other studies have focused on the understanding of microstructure formation and their interpretation (Hiemstra and van der Meer 1997; Phillips et al. 2011, 2013; van der Meer and Menzies 2011; Menzies 2012; Menzies et al. 2016*a*; Spagnolo et al. 2016). However, few microsedimentological investigations of thick, continuous subglacial traction sediments (e.g., >10 m) have been undertaken, such as those inter alia by Phillips and Lee (2013), Menzies and Reitner (2016), Skolasińska et al. (2016), and Phillips et al. (2018). The examination of a thick succession of subglacial traction sediments, overlying relatively flat bedrock topography, offers the unique opportunity to develop insights into fluctuating stress levels in subglacial tills and their relationship to different till unit formation. Unique microstructures in subglacial tills appear to form by progressively increased stress levels (Menzies et al. 2016*a*). However, how changes in stress levels relate to subglacial sediment formation, and ice sheet dynamics, as well as how stratigraphically distinct till units develop, remain poorly understood. Microshears have been identified as good indicators of stress levels within till (Tchalenko 1970; Larsen et al. 2006*a*; Thomason and Iverson 2006; Menzies et al. 2016*b*) and will be utilized in this study to better understand changes in strain in relation to till unit separation.

A large section of subglacial sediments is exposed on the walls of a former open-pit (K-62) within the past-producing Pine Point lead–zinc mine, Northwest Territories, Canada. This exposure provided an opportunity to evaluate the changing deformational history of over 20 m of subglacial sediments. A perspective on subglacial tills is presented here based upon microsedimentological investigation. However, this research is coupled with macroscale sedimentological research that included clast microfabric measurements, grain size determination, and geochemical, heavy mineral, and clast lithology analyses (Rice et al. 2013). The development of microstructures in till has been attributed to variations in subglacial conditions, including clay content, porewater pressure, thermal fluctuations, and stress fluctuations (cf. Passchier and Trouw 1996; Tembe et al. 2010). As such, the relatively uniform grain-size composition throughout the units (cf. Rice et al. 2013), the relatively uniform subglacial conditions in this region of the Laurentide Ice Sheet (LIS), as inferred by multiple glacial models (Marshall and Clark 2002; Kleman and Glasser 2007; Tarasov and Peltier 2007; Stokes et al. 2012), and the apparent lack of abundant porewater escape structures (discussed below), make the lithofacies at open-pit K-62 ideal for studying the effects of varying stress levels on microstructure development and their relation to till unit separation.

In this paper, microscopic identification of stress-induced structures throughout four till units provide insights into different subglacial stress levels and their relation to till unit separation in the western sector of the LIS.

Location, quaternary geology, and previous work

The past-producing Pine Point lead–zinc mine site is located along the southern shore of Great Slave Lake, ~50 km east of Hay River, Northwest Territories (Fig. 1). In this region, a range of Quaternary sediments (discussed below) overlie Devonian carbonate rocks (Hannigan 2007). The open-pit examined in this study

(K-62) is located ~75 km west of the boundary between the Precambrian Canadian Shield and the Paleozoic Western Canada Sedimentary Basin (Fig. 1). The Quaternary geology of the mining district is the net effect of glaciation by ice of the LIS (Dyke et al. 2002) and the migration of the Keewatin Ice Divide throughout the Wisconsin glaciation (McMartin and Henderson 2004). Sections of glacial sediments up to 25 m thick are exposed in abandoned open-pits in the former mine (cf. Rice et al. 2013, 2014), with even thicker deposits in former bedrock karst collapse features (Lemmen 1990; Rice et al. 2013). Open-pit K-62 was selected for this study as it offered a continuous exposure of 22.4 m of glacial sediments overlying Paleozoic bedrock that could be safely studied in detail.

Early surficial mapping of the Pine Point area focused mainly on glacial Lake McConnell and its role during deglaciation of the Great Slave Lake region (Lemmen 1990, 1998*a*, 1998*b*; Lemmen et al. 1994), and mapped landforms that indicate a former ice flow phase to the west, which had been previously shown on the Glacial Map of Canada (Prest et al. 1968), compiled from early Geological Survey of Canada reconnaissance surveys. Through this work, Lemmen et al. (1994) described a single till unit at Pine Point. Subsequent work, using visual observations, grain size, till-matrix geochemistry, indicator mineral abundance, and pebble lithologies, identified four distinct till units at open-pit K-62 (Rice et al. 2013). Oviatt and Paulen (2013) and Oviatt et al. (2015) mapped striae exposed on the bedrock shoulders of the open-pits and identified three main ice flow phases which correlated with the regional ice flow pattern established from the geomorphological record in the area (Rice et al. 2013). These investigations identified the earliest flow phase was to the southwest (~230°), followed by a dominant flow phase to the northwest (~300°), and finally, a west–southwestward flow phase associated with ice streaming during deglaciation (~250°) (Fig. 2). Remote sensing investigations identified glacially streamlined features to the northwest, west, and southwest of Pine Point that denote the final ice-flow direction in the region (Lemmen et al. 1994; Winsborrow et al. 2004; Margold et al. 2015). As the ice margin retreated eastward, the Pine Point region was inundated by glacial Lake McConnell between 11.6 ^{14}C ka (Lemmen 1990) and 11.1 ± 1.1 ka (Oviatt and Paulen 2013). Wave erosion from the glacial lake winnowed the till surface and deposited thin (<2 m) beach and littoral glaciolacustrine sediments across the entire district (Lemmen et al. 1994; Oviatt and Paulen 2013). As the LIS retreated, anticyclonic wind circulation formed aeolian sand dunes on the raised beaches of glacial Lake McConnel prior to vegetation colonization during the early Holocene (Wolfe et al. 2004).

Methods

Macrosedimentological properties

To characterize the visual changes observed throughout the lithofacies (Fig. 3) a series of 3 and 20 kg samples were collected throughout the vertical facies. The samples were collected after clearing any overlying surface debris slump, to reveal in situ till. The 3 kg samples were submitted to the Geological Survey of Canada's (GSC) Sedimentology Laboratory, Ottawa, for geochemical and grain-size analysis, as well as Munsell colour determination. Samples were split into three different aliquots for each analysis following procedures outlined by Girrard et al. (2004). One aliquot was dried at 105 °C for 15–30 min and disaggregated and Munsell colour determination was conducted using a Spectrophontometer link to iQC colour software. The grain-size analysis was conducted on a separate aliquot using a combination of wet and dry methods. The fraction >0.063 mm was determined by wet sieving and fractions <0.063 mm were determined using a Lecotrac LT-100 Particle Size Analyzer. An additional aliquot of <0.062 mm material was sent to Acme Labs, Vancouver, (now Bureau Veritas) for geochemical analysis by aqua regia digestion and ICP-MC determination (Group 1F package).

Fig. 2. Three different phases of ice flow recorded by striation measurements on bedrock shoulders of abandoned open-pits in the Pint Point mining district: (A) oldest flow phase (blue, 230°) and intermediate flow phase (red, 300°), and (B) intermediate flow phase (red, 300°) and youngest flow phase (black, 250°). Top left inset: zoomed in view showing details of striations. (C) SPOT satellite image of Highway 5, southwest of the Pine Point mining district, showing older large, northwest-trending landforms (red dashed arrows oriented 300°) crosscut by smaller southwest-oriented flues (black solid arrows 250°). [Colour online.]

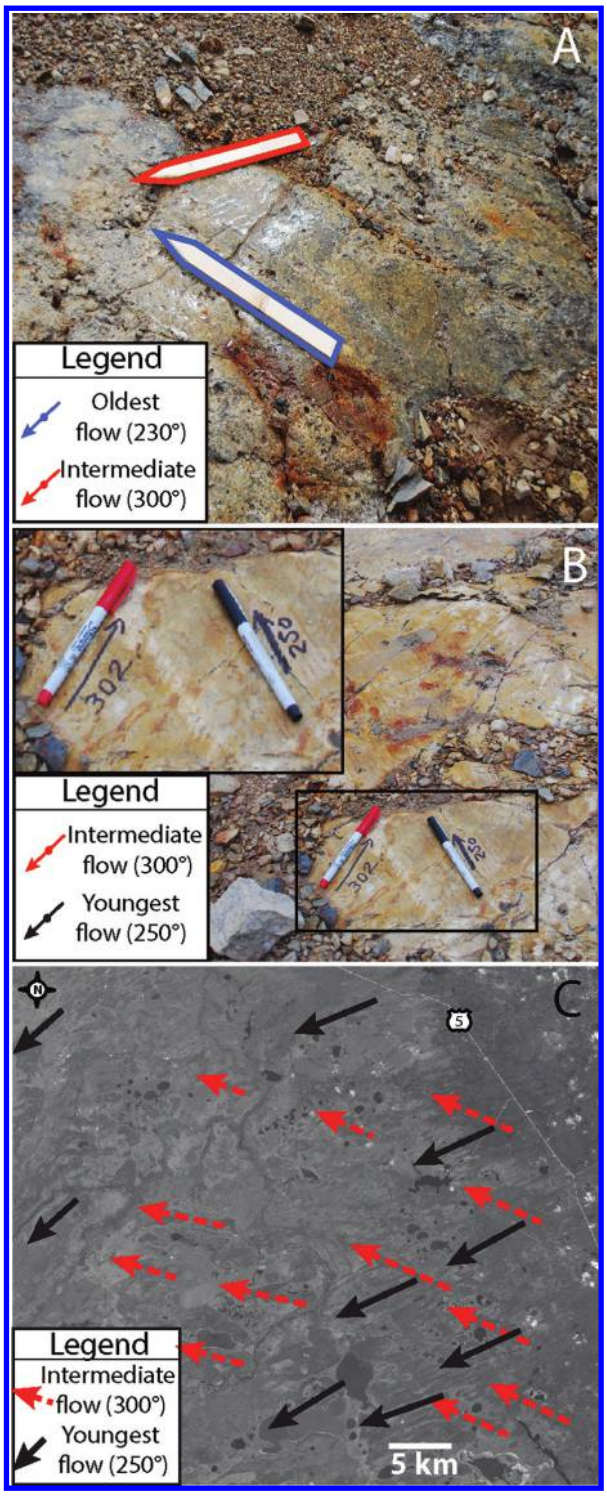

Fig. 3. North face of open-pit K-62 with annotations showing four till units (A–D) overlain by glacial Lake McConnell littoral sediments (Unit E), location of micromorphological and bulk till samples, and locations of till macrofabric measurements. The total vertical height of the section is 23 m. The dashed lines indicate the approximate contacts identified between till units. The red boxes indicate the locations of Figs. 5 and 7. [Colour online.]

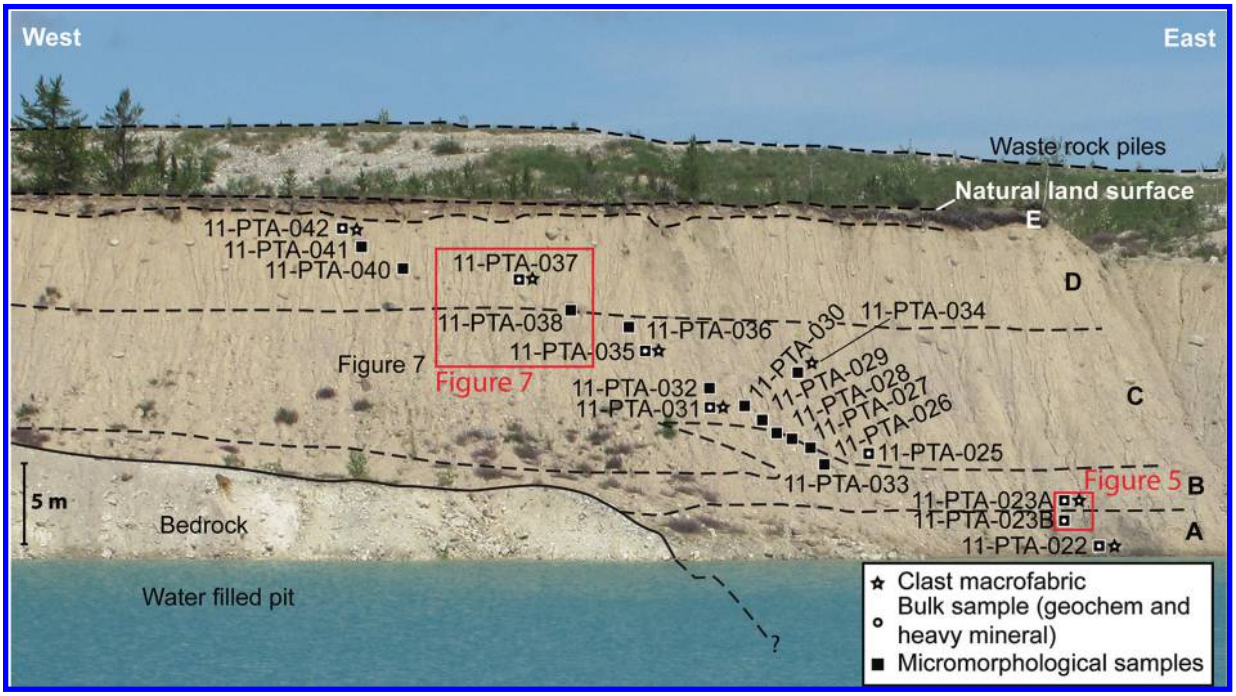

The 20 kg samples were submitted to Overburden Drilling Management Limited, Nepean, for disaggregation and heavy mineral identification and quantification. Each till sample was disaggregated in water then wet sieved to 2.0 mm, with the >2.0 mm till fraction washed with oxalic acid to remove iron staining and discolouration and retained for clast lithology analysis (see below). The <2.0 mm fraction was used for heavy mineral identification and counting, following protocols of the GSC (Plouffe et al. 2013).

Clast lithology analysis

To characterize the changing sediment provenance throughout the vertical facies, seven bulk sediment samples (20 kg) were collected for clast lithology determination. The sub-cropping margin of the Precambrian Canadian Shield with the western boundary of the Paleozoic Western Canadian Sedimentary Basin ~175 km east of the study site allows for discrimination between locally derived and far-travelled clasts. Clast lithologies allow for an inference of ice flow direction (i.e., down ice of the parent bedrock unit) and are used to discriminate between the different units within the facies using the relative percentages of each lithology (Trommelen et al. 2013). The >5.6 mm fraction of the bulk sediment samples (2–3 kg) yielded 800 to 900 clasts per sample. The clasts were well mixed by hand then coned and quartered to randomly select 300 to 400 clasts for lithologic sorting. Selected clasts were categorized as either Precambrian Shield or Paleozoic Western Canadian Sedimentary Basin based from bedrock lithologies within the Pine Point region and up-ice thereof (Skall 1975) to determine the general provenance of the till sample.

Till macrofabric analysis

To evaluate whether the erosional evidence (striation data) from the study area correlated to the depositional phase of ice flow, seven clast fabric measurements were conducted throughout the vertical facies (see Fig. 3 for fabric sampling locations). Till macrofabric measurements utilize the tendency of elongated clasts to develop a preferred shape alignment parallel to the dominant ice flow direction during deposition and accretion (Carr and Rose 2003; Hart et al. 2009). A horizontal bench was hand-dug into the diamict facies to conduct macrofabric measurements on a random selection of clasts (with an A:B axial ratio of ≥2:1) (Chandler and Hubbard 2008) within ~1 m^3 sample area, as recommended by Ringrose and Benn (1997). The angle of plunge and trend of each clast were measured along the a-axis for a minimum of 50 prolate clasts (elongation ratio of 2:1), with a minimum length of 20 mm (a-axis), at each of the seven sites following procedures outlined by Benn (2004). As this was microscale till analyses, only seven sites were selected based on the best accessibility and allowed appropriate time for all data collection.

Micromorphological samples

Undisturbed bulk samples and Kubiëna tins filled with sediment were collected from a vertically excavated till section, parallel to the exposed face, for subsequent thin section production (Fig. 3). Samples were collected from 18 sample sites within open-pit K-62—of these collected samples, a total of 46 thin sections were produced. A minimum of two thin sections per collected sample were produced, each cut parallel to each other separated 3–4 mm apart. Where the thickness of the collected sample permitted, a third thin section was produced, which resulted in the 16 thin section "sets" presented in this study. The thin sections were manufactured from a vertically cut face (vertical to the collected horizon) from each collected sample, ensuring the original sample azimuth was also preserved. Where the sediment in Kubiëna tins could not be collected due to the fissility, overconsolidation, or higher clast content of the diamict, tins partially filled with sediment were collected and then backfilled with well-sorted medium-grained sand. For a detailed description of field sample collection see Rice et al. (2014). Each sample was vacuum-sealed after collection and shipped to Brock University.

Micromorphological samples were processed by the Brock University petrographic laboratory, St. Catharines, Canada, using methods outlined in Murphy (1986) and subsequently summarized by Menzies and van der Meer (2018). Analysis of thin sections

Table 1. Macrosedimentological characteristics of collected samples.

Sample No.	Till Unit	Depth from land surface (m)	Munsell Colour (wet)	Description	Clast content (%)	% Sand (0.063–2.0 mm)	% Silt (2–63 μm)	% Clay (<2 μm)	Canadian Shield clasts (%)	Carbonate clasts (%)
PTA-022	A	17	10YR 6/2	Light brownish grey matrix, weak fissility, sand lenses	13	58.2	35.9	5.9	n/a	n/a
PTA-023B	A	16.2	5Y 5/2	Olive grey matrix, weakly fissile	8	39.2	49.2	11.6	61.4	38.6
PTA-023 A	B	16.1	10YR 7/2	Light grey matrix, iron stained clasts	13	32.0	49.6	18.4	29.8	69.9
PTA-025	C	12.5	10YR 6/2	Light brownish grey matrix, sand rich	11	33.7	48.1	18.1	n/a	n/a
PTA-030	C	9.8	10YR 7/2	Light grey matrix, sand rich	16	34.9	47.6	17.6	32.6	67.4
PTA-035 A	C	6.2	10YR 6/2	Light brownish grey matrix, strong fissility, clay rich	17	33.4	48.0	18.6	25.1	74.9
PTA-037	D	4.2	2.5Y 7/2	Light grey matrix, with iron staining on joints	12	30.8	50.1	19.1	22.6	77.4
PTA-042	D	1.2	2.5Y 7/2	Light grey matrix, strong fissility	18	34.5	49.8	15.6	19.2	80.5

Table 2. Indicator mineral data from collected samples (summarized from McClenaghan et al. 2012).

Sample No.	Till Unit	Pyrite/Marcasite	Chalcopyrite	Galena	Hercynite	Kyanite	Sillimanite	Starolite	Sphalerite
PTA-023B	A	3333	0	0	4	167	167	7	80
PTA-023 A	B	2041	1	10	14	14	27	1	272
PTA-030	C	2128	0	21	0	4	7	0	284
PTA-035	C	2256	1	8	2	2	113	1	75
PTA-037	D	7	0	5	15	41	7	1	3
PTA-042	D	16	0	0	3	62	0	0	0

was conducted at low magnification (6.5×–10×) in plain and cross-polarized light using a Wild-Heerbrugg® M420 microscope affixed with a Nikon® Digital sight and an SD-Fil digital imaging device. Composite images of thin sections were compiled using Nikon® NIS-Br imaging software, and subsequently, microstructures were annotated. Once the initial microscopic analysis was complete, thin sections were placed on a PetroScope® projection macroscope under plain light (2×) and re-analyzed to confirm the identification of structures and aid in the identification of any larger structures not recognized through microscopic analysis.

Microshears (lineations) have been identified as ideal microstructures for recording stress levels within the till (Tchalenko 1970; Larsen et al. 2006*a*; Thomason and Iverson 2006; Menzies et al. 2016*b*). Additionally, experimental ring-shear testing has demonstrated that shear structures become increasingly parallel to the direction of strain with increasing strain (Larsen et al. 2006*a*). Research has shown that the angle of microshears can be classified as symptomatic of low strain if they are >25° and high strain if they are <25° (Morgenstern and Tchalenko 1967; Tchalenko 1968).

In this study, microshear orientation was measured relative to the natural land surface and plotted on rose diagrams. In measuring microshear angles, great care was taken to cut the sediment as a vertical thin section parallel to the dip direction of the clast macrofabric measured in the field and thus parallel to ascribed ice flow direction of the macrofabric. The recognition of microshear structures in two-dimensional thin sections is not a simple task. Detection of these microstructures, likely caused by microscale movement along the sides of such shear displacement and, in some places, evidence of a downthrown side, indicates the presence of microshears. Essentially along these shears, the internal cohesion has been destroyed or disrupted. Most of these microshears within subglacial tills are either shear-fracture or slip planes (Hills 2012). The results should be interpreted with caution and only give a sense of the degree of stress involved, not the direction of the stress (Menzies and Reitner 2016). Larsen et al. (2006*b*), Thomason and Iverson (2006), and Narloch et al. (2012) used an IL Index of cumulative length of low-angle microshears measuring shear length and orientation on two-dimensional microshears. However, the present authors believe there is too much possible error in the adoption of the IL Index, specifically in terms of using shear length as a measure, since in many cases, only partial sections of any given microshear can be observed in a single thin section (cf. Phillips et al. 2013, 2018). To address this problem of perception, only the specific number of low-angle microshears as a percentage of high-angle microshears is considered acceptable as data in the present investigation. Because a thin section is a two-dimensional representation of a three-dimensional object, a series of parallel thin sections were cut no more than 3–4 mm apart, such that juxtaposed thin sections could be visually compared as a single set for one sample (Fig. 4). Using these sets allows for the two-dimensional presence of microshears to be detected in the third-dimension. Sets of microshears that were not evident in other parallel thin sections were not used.

Macrosedimentological results and interpretations

Lithostratigraphic units

Results from all analytical methods are listed within the unit from which they were collected below. Complete Munsell colour and grain size results are reported in Table 1. Select heavy minerals and geochemical results are reported in Table 2, with full results available from the GSC (McClenaghan et al. 2012; Oviatt et al. 2013*a*, 2013*b*). Clast macrofabric results are presented in Table 3. All the till units were matrix supported, overconsolidated, and contained sub-rounded to sub-angular clasts, many of which were striated and faceted.

Unit A

This unit is the lowest unit at open-pit K-62 and is found primarily within a karst bedrock depression and also occurs as thin, flat-lying discontinuous lenses on the bedrock surface down ice-flow (west) from the karst depression. Only 1 m of this unit was exposed above water level within the open-pit; thus, the total thickness of this unit is not known. However, in July 2017, an exploration diamond drill hole (EX-17-DBL-003) ~2 km south of open-pit K-62 intersected up to 10 m of similar diamicton (pers.

Table 3. Macrofabric data.

Sample No.	Till Unit	Depth from surface (m)	n	Eigenvalues S_1	S_2	S_3	Isotropy index	Elongation	Shape
PTA-022	A	17.0	51	0.47	0.35	0.18	0.39	0.25	Girdle/Isotropic
PTA-023 A	B	16.1	63	0.54	0.36	0.10	0.19	0.33	Girdle/Cluster
PTA-031	C	9.0	51	0.77	0.18	0.05	0.06	0.76	Cluster
PTA-034	C	7.2	50	0.65	0.23	0.12	0.19	0.64	Cluster
PTA-035	C	6.2	53	0.69	0.25	0.05	0.08	0.63	Cluster
PTA-037	D	4.2	52	0.61	0.27	0.13	0.21	0.56	Cluster
PTA-042	D	1.2	52	0.68	0.27	0.05	0.08	0.61	Cluster

Note: Isotropy index: $I = (S_3/S_1)$ (Benn 1994*a*, 1994*b*). Elongation: $E = (1 - (S_2/S_1))$ (Benn 1994*a*, 1994*b*). Shape (Benn 2004).

Fig. 4. Outline of methodology for producing thin sections perpendicular to ice-flow direction, cutting multiple thin sections from a single sample to allow the measuring of shear structures throughout the sample. [Colour online.]

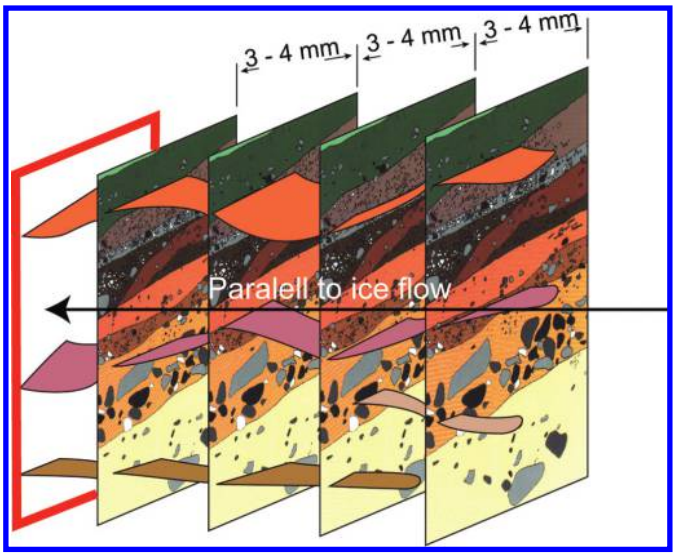

comm., S. Clemmer, Pine Point Mining Limited, 2017). Unit A is matrix supported, olive grey (10YR6/2-wet) with a silty-sand matrix (58% sand; 36% silt), and a clast content of ~13%. Clasts collected from this unit are mostly (61%) Precambrian Canadian Shield lithologies (Table 1), with lower percentages (39%) of the local Paleozoic carbonate lithologies. Similarly, indicator mineral results show elevated counts of kyanite, silmanite, and pyrite, but lower counts of sphalerite, galena, and hercynite than overlying Unit B. A single clast macrofabric measurement was conducted on this unit and yielded a polymodal fabric (Hicock 1991) with no clear orientation (Table 3). Unit A is fissile throughout and contains several sorted sand lenses.

Unit B

This unit is an aerially extensive unit observed in the lower parts of many open-pits throughout the Pine Point region, where it is observed overlying bedrock surfaces and Unit A till in karst depressions. At open-pit K-62, Unit B averages 2.5 m thick, is matrix supported, and has a light grey (10YR 7/2-wet) sandy-silt matrix (32% sand; 50% silt) with a clast content of 13%. Clasts collected from this unit contained only 30% Precambrian Canadian Shield clasts and 70% of more local carbonate clasts (Table 1). The lower portion of Unit B contains rip-up or reworked "rafts" of underlying Unit A diamict that have been incorporated, but not completely homogenized, into Unit B (Fig. 5). Indicator minerals identified from this unit imply a clearly different provenance

Fig. 5. Deforming contact and mixed units between Unit A and Unit B. Rip up clasts from Unit A can be seen preserved within Unit B. Canadian five-cent coin (21.2 mm) for scale. [Colour online.]

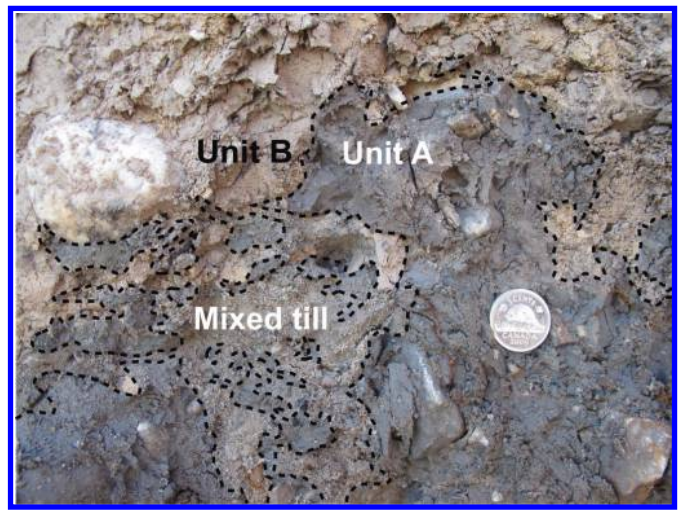

than underlying Unit A, but a similar provenance to overlying Unit C (Table 2). Clast macrofabrics measured directly above the deformational contact suggest an ice flow azimuth of ~290° (Table 3) with a bimodal distribution and isotropy index (S_3/S_1 = 0.19) indicative of a clustered fabric (Fig. 6).

Unit C

This unit is 12 m thick, making it the thickest unit observed within open-pit K-62 (Fig. 3). It has a brownish grey (10YR 6/2-wet) sandy-silt matrix (34% sand; 48% silt) with an average clast content of 11%–17%. Clast content within Unit C increases from the bottom towards the top of the unit from 11% in the lowest sample to 17% in the highest sample. However, matrix texture does not vary more than 1.5% (Table 1), containing 25%–33% Precambrian Canadian Shield lithologies and 67%–75% local carbonate lithologies. Indicator mineral results denote a similar provenance to underlying Unit B; however, the abundance of indicator minerals, excluding kyanite, are all much higher than overlying Unit D (Table 2). A deformational contact defines the contact between Unit B and Unit C. Macrofabric results show clasts are clustered in a generally parallel direction to each other (Table 3; S_1 = 0.65–0.77). Macrofabric from this till unit all display a bimodal distribution (Fig. 6) with similar inferred ice flow azimuths (230–270°) that are similar in orientation to striations on local bedrock outcrops and streamlined glacial landforms in the area (Fig. 2; Table 4).

Unit D

This unit is the uppermost unit (2.5 m thick) and consists of light brownish grey (2.5Y 7/2-wet) sandy-silt matrix (33% silt; 50%

Fig. 6. Ternary plot showing the shape distribution based on eigenvalues calculated from a-axis fabric data from each unit, with Unit C and Unit B having the strongest clustering, Unit B having a more girdle shape, likely indicative of overprinting, and Unit A having no clearly defined shape, plotting almost in the center of the diagram (Benn 2004). Equal area stereoplots with Kamb contouring for each macrofabric with interfered ice flow direction are included following recommendations by Hicock et al. (1996). [Colour online.]

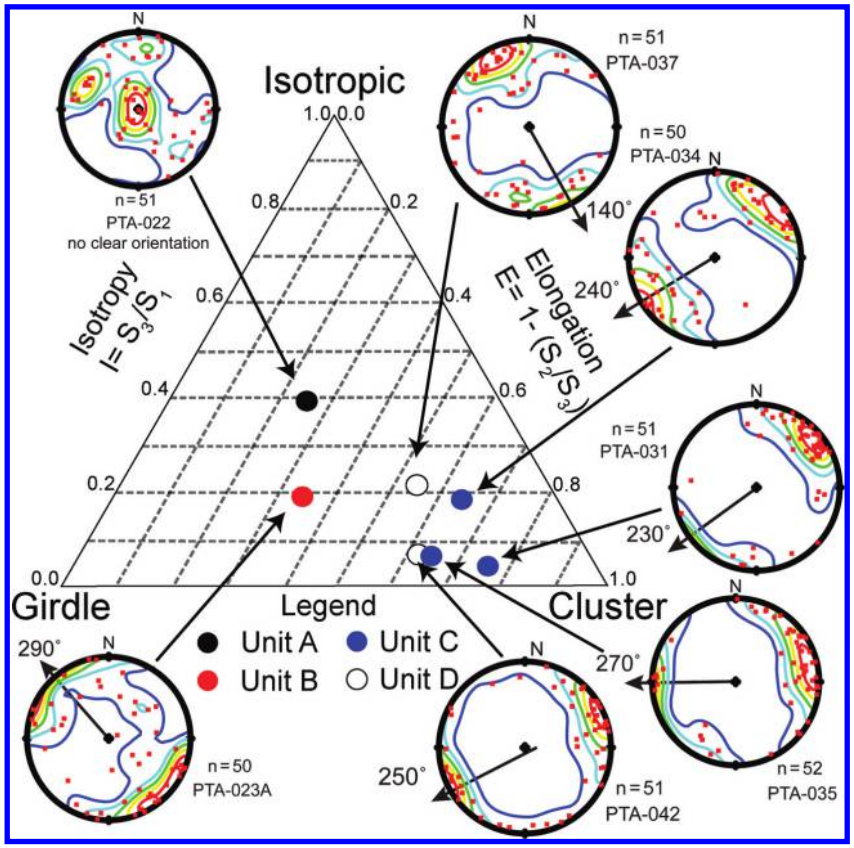

Table 4. Ice flow indicator summary.

Macrofabric	Till Unit	Striae	Landforms
250°	D	250°	250°
140°		330°	
270°	C	300°	300°
240°			
230°		230°	
290°	B		
?	A		

sand) diamicton containing 17% clasts. Clasts within this unit were 19%–23% Precambrian Canadian Shield lithologies and 77%–81% more local carbonate lithologies. Indicator mineral abundances are much lower in this unit; however, they have higher counts of kyanite. A boulder horizon defines the contact between Unit C and Unit D (Fig. 7) and is comprised of moderately sized boulders (average a-axis of 0.6 m) some of which are faceted, and many are striated on all sides and have been polished. No preferred striation direction was observed on the upper surface of the boulders. Macrofabric measurements within this unit vary slightly (Table 3; Fig. 6). The lowest macrofabric measurement (PTA-037) has a bimodal distribution, which implies an ice flow to the southeast (140°, S_1 = 0.61). However, the macrofabric measurement taken near the top of the unit (PTA-042) indicates an ice flow event to the southwest (250°, S_1 = 0.68). The upper macrofabric results show an ice flow trend similar to the fine elongated glacial landforms observed in the study area and striation measurements on exposed bedrock outcrops (Fig. 2; Table 4).

Unit E

This unit consists of littoral beach sediments (<2 m thick) deposited during the development of glacial Lake McConnell (Lemmen et al. 1994; Smith 1994; Oviatt and Paulen 2013). The proglacial lake winnowed Unit D's surface and deposited littoral sediments that are characterized by large sub-rounded cobbles and boulders of similar lithologies to Unit D, with an open framework coarse sand matrix. In lower-lying areas, these glaciolacustrine sediments are covered by a deposit of peat ranging from 0.5 to well over 2 m in places.

Microsedimentological results and interpretations

Microstructures identified in thin section are outlined in Fig. 8 following the methods and interpretations of van der Meer (1993), Carr (2004), and Menzies (2000). It is understood that sediment rheology can be inferred from the character of the microstructures (cf. Menzies et al. 2016*a*; Phillips et al. 2018). It should be noted that the vug-like void features observed in the samples were likely formed during the production of the thin sections, as fracture voids—the result of the drying process (Carr 2004). Although

Fig. 7. (A) Oblique image defining the boulder horizons at the contact between Unit C and Unit D. (B) Gradational contact between Unit C and Unit D displaying the subtle difference in till colour (boulders removed before photographing). Boulder contact has faceted and striated boulders along a semi-continuous horizon. The handle of the pick is 60 cm. [Colour online.]

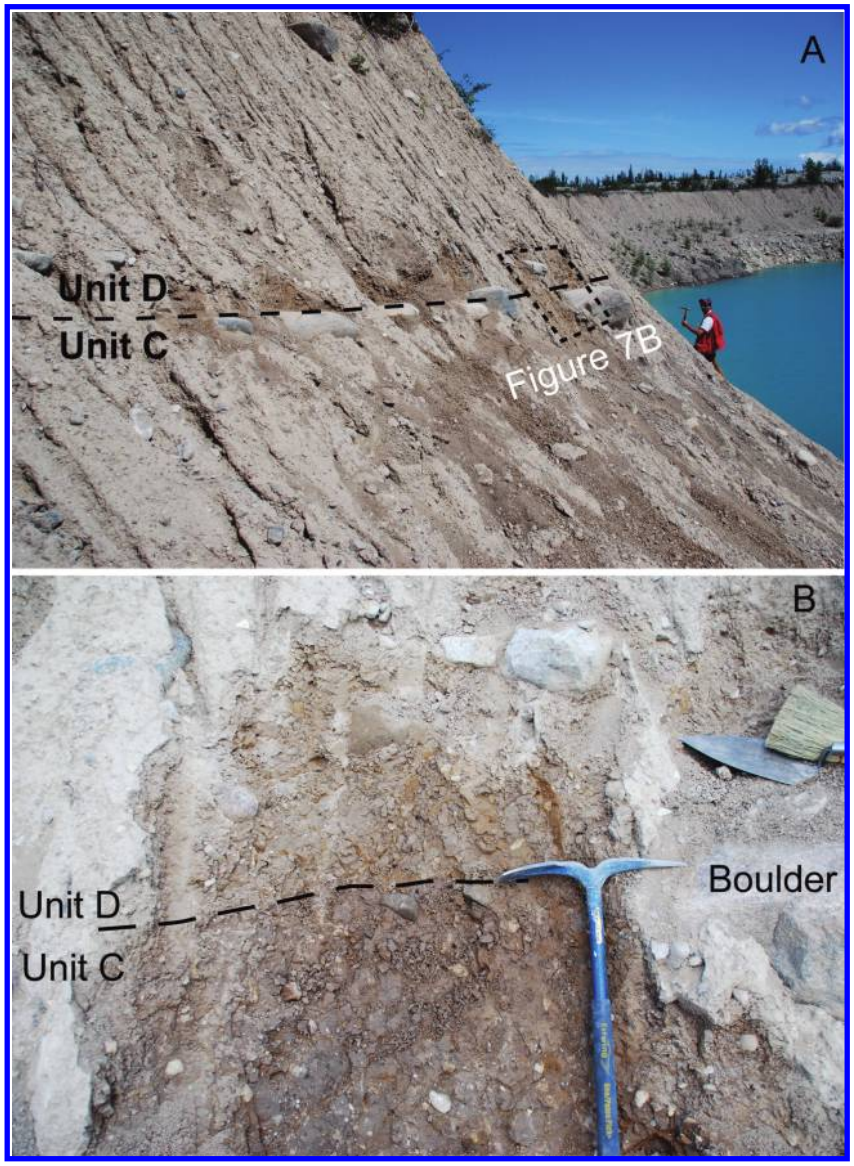

these voids may highlight weaknesses within the matrix, they do not directly reflect subglacial processes.

Unit A

Microstructures identified from the two samples collected from this unit (PTA-022 and PTA-023B) include rotation structures, high and low angle microshears, and grain stacks. The lower of the two samples collected from this unit (PTA-022) contains a greater abundance, by simple visual inspection, of sand-sized grains than other samples collected throughout the section (Fig. 9A; Table 1). The presence of rotation structures is evidence of ductile deformation of the sediment; however, there are few rotation structures within the lower section of the till unit (Fig. 9A compared to 9B). The rotation structures do not crosscut the microshears, making their age relationship difficult to establish; however, the multiple orientations of microshears suggest brittle deformation of the sediment happened in multiple phases.

Unit B

A sharp contact is observed between Unit A and overlying Unit B (Fig. 9B), within which intraclasts of Unit A have been incorporated into Unit B can be identified (dashed outline). Only one sample was collected from Unit B as this unit was not thick enough to collect additional samples. Microstructures identified from samples in this unit (PTA-023A; Fig. 10) include high and low angle microshears, rotation structures, grain stacks, and microfractured and fragmented grains, all indicate that ductile and brittle deformation processes affected the diamicton likely as a function of porewater content and fluctuating stress levels (Fig. 10). The presence of multiple domains (defined as areas of slightly different or, in some cases, very different lithofacies units that have all been "incorporated" into a sediment package (cf. Menzies et al. 2016*a*)) within the sediment demonstrates that parts of Unit A were reworked and incorporated into Unit B, but that the process of intermixing did not completely homogenize the two till units. The abundance of rotation structures indicates high levels of matrix deformation as the two till units mixed (Jørgensen and Piotrowski 2003).

Unit C

Although this unit is the thickest (12 m), the microstructures throughout the unit are similar to the suites of microstructures

Fig. 8. Legend of deformation structures identified in thin section, indicative of descending intensity of stress levels over time on the left and other micromorphological structures identified on the right (Menzies 2000; Ravier et al. 2014*a*; Menzies et al. 2016*b*). Edge-to-edge crushing begins at the onset of stress as larger grains are forced against one another. As stress levels increase, grain stacks (grains that line up along a singular plane) and microshears or lineations (discontinuities) (readjustment of the clay fraction of the matrix appearing as a thin line) form, becoming increasingly parallel to the direction of increasing stress levels (Menzies et al. 2013, 2016*b*). With increased subglacial shearing, rotation structures will form and are characterized by the rotation of matrix and fine-grained material within the till. As shear increases, deformation bands (thin zones of fine-grained sediment in relatively clay-rich zones (Gao et al. 2012; Menzies et al. 2013)) will form, eventually leading to separate domain formation, whereby, different diamict matrices have been incorporated, but not completely homogenized, likely from previously deposited sediments (cf. Truffer et al. 2000; Jørgensen and Piotrowski 2003; Boulton 2006). Additionally, voids are gaps within the matrix, either as pore spaces or created during the production of the thin sections (Carr 2004). Necking structures are v-shaped alignments of fine-grained material being squeezed through a gap between larger clasts. Clay accumulations are associated with elevated local porewater, which created localized elevated porewater pressure, leading to the formation of low strain clay accumulations or bands. Additionally, clasts are undifferentiated pebbles found throughout the thin section. Porewater draining structures indicate porewater has flushed some of the fines, leaving coarser-grained material. There porewater draining structures are commonly associated with clay accumulations. Finally, the "sand packing" is fine sand used to pack unfilled spaces in Kubiëna tins prior to shipping to minimize disturbance of the collected samples (cf. Rice et al. 2014). [Colour online.]

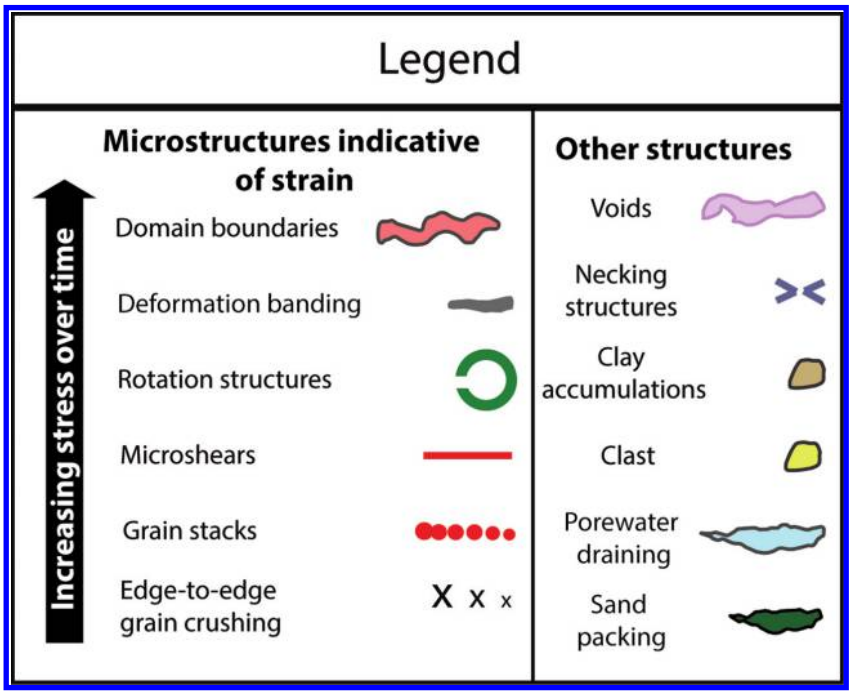

identified from samples collected in other units. Eleven micromorphological samples were collected from this unit (Fig. 3); five of which (samples PTA-025 to PTA-029) were sampled along the lower contact with Unit B and contain similar micromorphological characteristics to PTA-028. For the sake of brevity, the annotated versions of the remaining samples (PTA-025, PTA-026, PTA-026, PTA-027, and PTA-029) are not reported here, but those images were published in Rice et al. (2014). The most abundant structures identified within this unit are rotational structures, microshears, fracture voids, necking structures, and crushed grains. Other microstructures observed include deformation banding (Fossen et al. 2017) (Fig. 11A) and water escape structures associated with clay cutans (Fig. 11B). Multiple domains can be identified in most of the samples taken from this unit, which implies that some of Unit B was re-worked and incorporated into Unit C throughout deformation and deposition, but the units were not fully homogenized. Microshears observed in the sediment transcend both domains, this indicates that the external stress that created these microshears occurred after the mixing of the two units.

The sample collected closest to the contact between Unit B and Unit C (sample PTA-30; Fig. 11B) contains a water escape structure with clay cutans. Two other samples (PTA-031 and PTA-032; Figs. 12A and 12B) were sampled several decimeters above this sample (Fig. 3) but did not contain water escape structures. The remaining samples from Unit C (PTA-035 and PTA-036; Figs. 13A and 13B) (PTA-038; Fig. 14) were also collected above the shear contact, within 2 m of the contact with overlying Unit D. Most grain stacks identified in thin sections from this unit are parallel to measured microshear orientations, possibly suggesting a sustained consistent stress level in the down-ice direction during deformation. Apart from the water escape structure identified from the sample above the deformational contact (PTA-030; Fig. 11B) and the shear bands identified from the sample just below the deformational contact (PTA-028; Fig. 11A), all the microstructures within this unit are nearly identical. The presence of a boulder horizon, change in till colour, and an increase in fissility mark a planar contact between Unit C and Unit D (Fig. 7). Unfortunately, sample PTA-034, collected midway between PTA-032 and PTA-035 was damaged during transportation to the laboratory and no analysis could be completed.

Unit D

This unit shows signs of considerable post-depositional disruption, possibly by pedogenic processes, freeze–thaw, and (or) other land surface impacts such as heavy equipment operation during the development of the open-pit, which is evident by the presence of abundant voids (cf. van Vliet and Langhor 1983). The lower two samples from this unit (PTA-037 and PTA-040; Figs. 15A and 15B) do

Fig. 9. Annotated thin sections from Unit A: (A) PTA-022 contains more fine-grained material within the matrix in comparison to other samples. Both samples contain rotation structures, microshears, and grain stacks. (B) PTA-23 shows the contact between Unit A (bottom of slide) and Unit B (top of slide), notice the inclusions of Unit A being incorporated into Unit B (black dashed outline). Rotation structures in the lowest sample from this unit (PTA-022-A) are much less abundant than in the uppermost sample (PTA-023). [Colour online.]

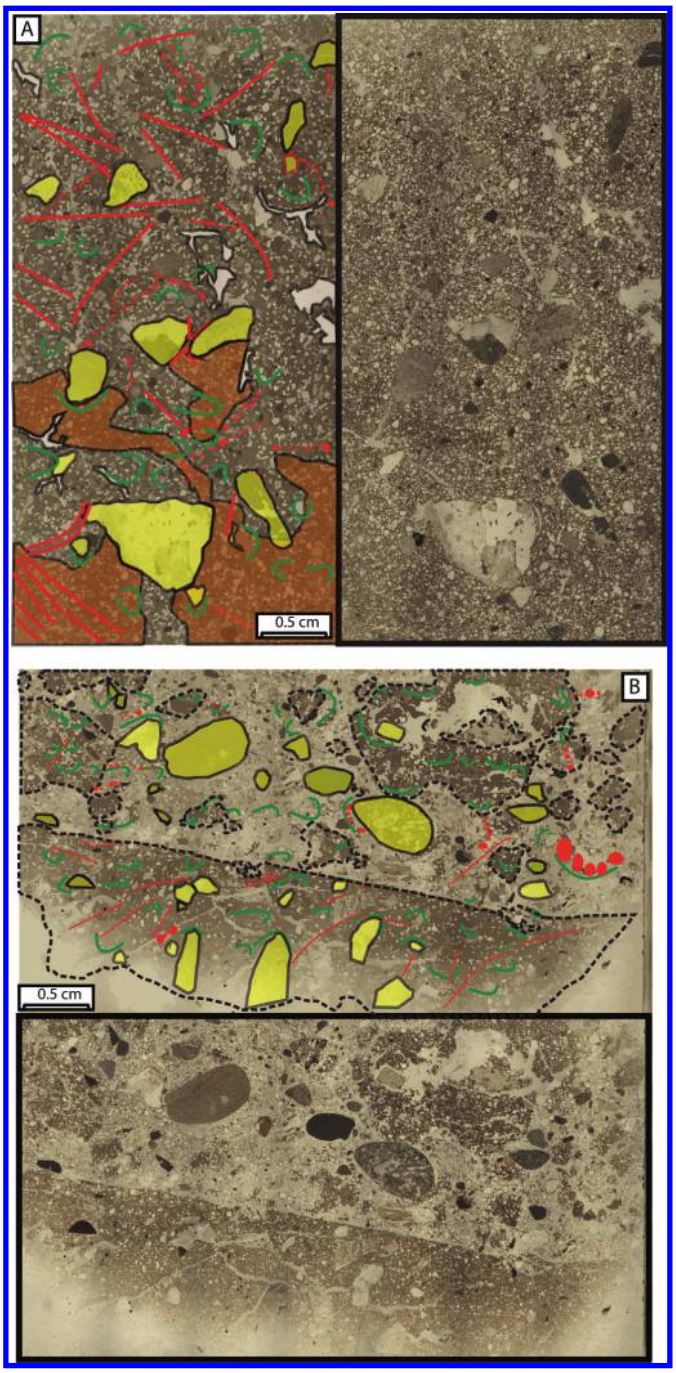

not contain an abundance of voids and were deemed reliable for analysis. These two samples exhibit high and low angle microshears, rotation structures, and crushed grains, with voids present in each thin section. Voids appear more abundant in PTA-040 (Fig. 15B) than the lower PTA-037 (Fig. 15A). The evidence for relative stress in the down-ice direction on these samples fluctuates

Fig. 10. Annotated thin sections from Unit C: PTA-023A with rotation structures, grain-stacks, microfractured and fragmented grains, and microshears. Evidence of multiple domains, indicating incomplete homogenization of Unit A incorporated into this unit (see Fig. 9B). [Colour online.]

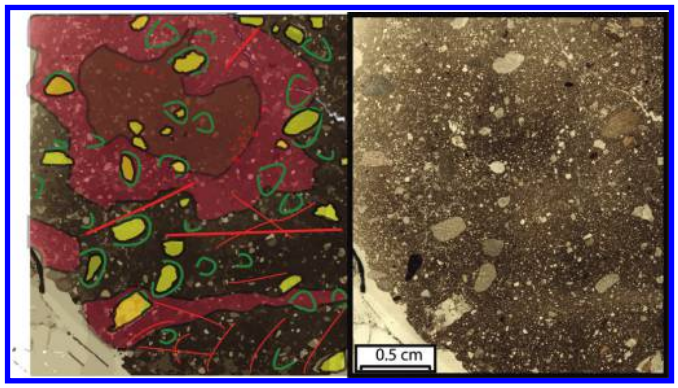

from high stress to low stress progressing vertically upward within Unit D, as indicated by the abundance of low-angle microshears observed within this unit (Fig. 16).

Microsedimentological interpretations

Microsedimentological examination confirms that the samples taken from each unit coincide with the macroscopic field observations of Rice et al. (2013). That is, the field interpretation of poor- to non-sorted, overconsolidated, fissile diamict units with abundant striated and faceted clasts as a subglacial advection sediment (till) is supported by the micromorphology (van der Meer et al. 2003; Carr 2004; Larsen et al. 2006*b*; Piotrowski et al. 2006; Phillips et al. 2008; Menzies and Ellwanger 2011). The lack of tiling structures within the matrix, admittedly negative evidence and thus not strong, typically associated with slump or debris-flow deposits (Lachniet et al. 2001; Menzies and Zaniewski 2003; Phillips 2006; Menzies and Whiteman 2009) was not observed in produced thin sections. This coupled with the preservation of increasing and (or) decreasing vertical fissility planes indicate that the samples were collected from in situ subglacial till and not from sediments remobilized by post-depositional slump wherein such planes would likely be absent or geometrically distorted.

Unit separation and ice flow chronology

Throughout the exposed section (Units A–D) there is microsedimentological evidence of ductile deformation as noted by rotation structures, grain stacks, and fluctuating abundances of reworked material (multiple domains), as well as evidence of brittle deformation indicated by multiple instances of crushed grains and microshears (Menzies 2000). The presence of these microstructures, coupled with in situ striated and faceted clasts, poor grain size sorting, the presence of subrounded, exotic macroclasts derived from considerable distance, the majority having strong clast macrofabric trends (cluster shape, whereby $S_1 \gg S_2 \approx S_3$) (Benn 2004), and a lack of any interglacial deposits between or within any of the units analyzed, implies that these sediments have been deposited as subglacial tills by accretion of a continuous, time-transgressive deforming bed.

Till unit separation between Unit A and the overlying units is the most distinct, with clear geochemical, mineral, and grain size differences from the overlying units (Tables 1 and 2). The pebble lithologies also suggest a different provenance for Unit A than the other units. Although the clast fabric yielded no definitive vector, the high abundance of Precambrian Canadian Shield clasts suggests a source to the northeast (Fig. 1). The separation of other units is less clear at the macroscale, largely due to a degree of reworking during till deformation and emplacement (see subgla-

Fig. 11. Annotated thin sections near the shearing contact between Unit B and Unit C: (A) PTA-028 contains a shearing band in the top left corner (green shading) and also contains abundant rotation structures and multiple domains. (B) PTA-030 contains water escape structure (blue) and associated clay accumulations and clay cutans (brown). [Colour online.]

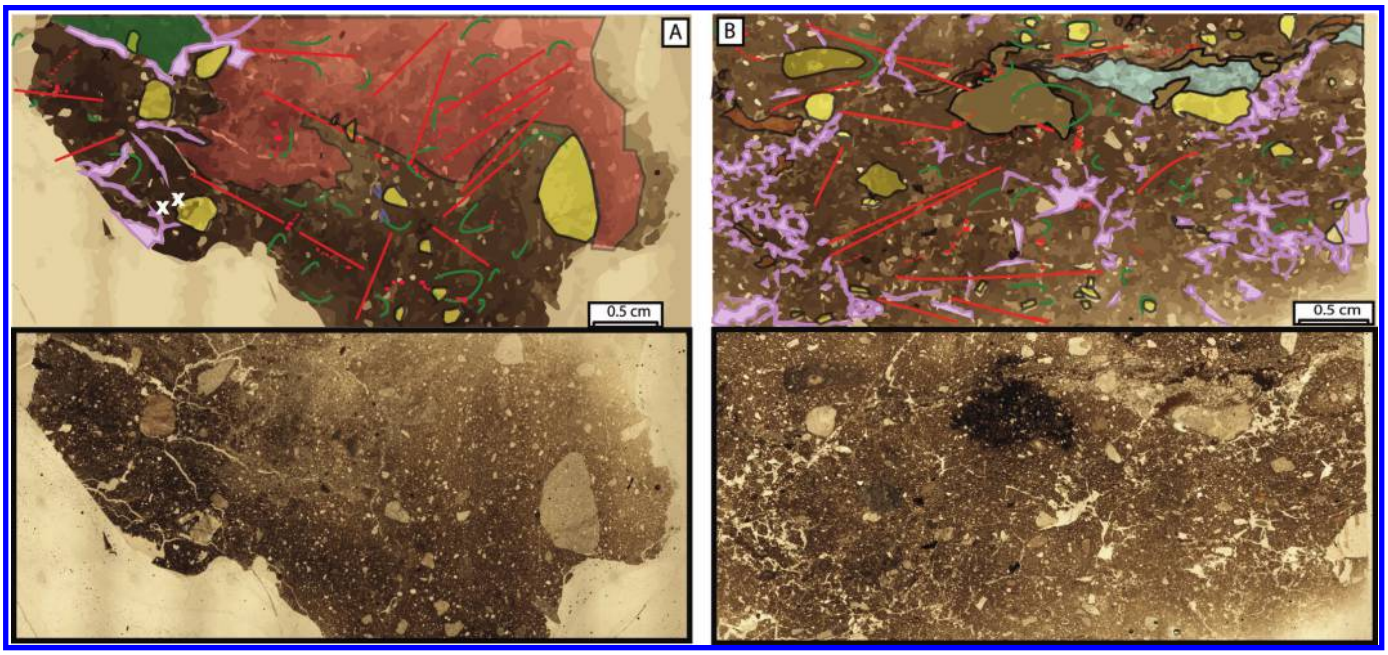

cial conditions through till emplacement). However, differences in clast fabric measurements (Fig. 6) suggest different ice flow events were responsible for each unit. Additionally, the slight differences in colour of the till units and the contacts identified between the units confirm the segregation of the four till units. Although Unit D has geochemical and indicator mineral abundances that differ from underlying Unit C, however, these differences may be the result of weathering processes breaking down the indicator minerals more susceptible to oxidation and altering the geochemical signature of the unit (Shilts and Kettles 1990), further investigation on the indicator grains would be required to confirm this. However, we interpret the boulder horizon between Unit C and Unit D as being the result of a viscous deformation event during the deformation and emplacement of Unit D (Hicock 1991), further justifying the separation of these units.

Four ice-flow phases were identified through till macrofabric analysis that correlates well with the erosional record around the Pine Point mining district (Table 4; Oviatt and Paulen 2013; Oviatt et al. 2015). This confirms the glacial history of the Pine Point region is much more complex than previously reported (Lemmen et al. 1994).

Subglacial conditions through till emplacement

Microstructures indicate the tills were emplaced subglacially under a temperate, wet-based active ice sheet as the deforming layer gradually became immobilized, causing fluctuations in basal ice strain, porewater pressure, temperature, and rheology of the subglacial deforming layer (van der Meer et al. 2003; Boulton 2006; Menzies et al. 2006; Phillips et al. 2018). These changes in deformational shearing have been attributed to changes in subglacial stress conditions within the deforming layer (Menzies et al. 2016*a*).

The angle of microshears relative to the main direction of principal stress, as indicated from the clast fabric's dominant azimuth, provide insights into how the changing subglacial stress levels correlate to known sedimentological properties (sedimentological characteristics, microstructures, clast fabrics, etc.) and the basal ice flow environment (striae and streamlined landforms). From this investigation, patterns emerge that reflect deformation of the till between the units, which denotes changes in subglacial conditions during and following till emplacement and accretion (Menzies et al. 2018). The plot of microshear angle abundances (Fig. 16) shows that the likely changes reflected in shear stress within the sediment packages are presumably a function of the stress level changes within sediment packages (cf. Fossen et al. 2018). As strain accumulated heterogeneously within a deforming region, dependent on strain intensity and geometry flow parameters, microstructures developed, evolved, or in some cases were overprinted or destroyed. These changes in stress affected the soft deforming till during emplacement, which caused them to become less mobile and resulted in deposition atop the immobile material (Menzies et al. 2016*b*). Iverson et al. (1998) describe similar mechanics during ring-shear studies of clay-rich tills in which shear zones experience a reduction in porewater pressure during shearing, strengthening the shear zone through "dilatant hardening", possibly acting as the mechanism from which the deformational layer becomes the immobile layer.

Several significant patterns are observed from the plotted changes in shear angle per cent abundances in the tills. A reduction in low shear angle abundance is observed at each till unit boundary contact with the overlying unit (Fig. 16). The zones where shearing has occurred appear to be related, to some extent, with changes in till units (i.e., between Unit A and Unit B). These changes in shearing location and abundance may indicate till sub-units being emplaced as individual immobilized layers as stress levels at the subglacial ice–bed interface fluctuated from low stress (immobilization of the deforming layer) to higher stress (mobilization of the deformable layer). This pattern can be clearly seen in the transition from Unit B to Unit C (Fig. 16). Below this contact, the shear angles fluctuate at about 35%–40%, however in sample PTA-028, just below the transition to Unit C, there is a distinct decrease (20%) in high angle microshear abundance. This fluctuation possibly indicates that Unit B evolved from an immobile unit that had undergone high stress level deformation into a re-deforming layer during the deformation and deposition of overlying Unit C. This pattern is again observed in the transition from Unit C into Unit D, where there is a small decrease in average

Fig. 12. Annotated thin sections from Unit C: (A) PTA-031 and (B) PTA-032, collected just above the shear structure associated with the boundary between Unit B and Unit C. These samples show less signs of shearing (no deformation bands) and have abundant rotation structures and microshears. Multiple domains indicating incomplete homogenization of the till unit can be observed in both samples. [Colour online.]

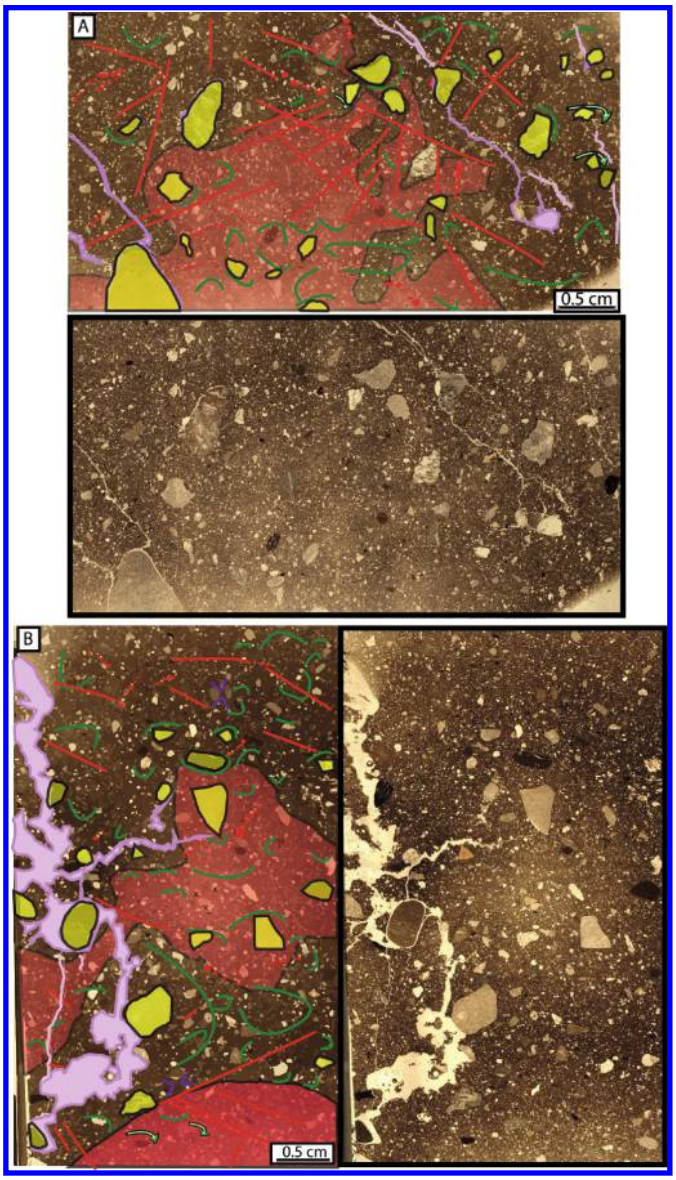

Fig. 13. Annotated thin sections from Unit C: (A) PTA-035 and (B) PTA-036, collected at the uppermost section of Unit C (Fig. 3). These samples contain rotation structures, grain stacks, microshears, and multiple domains. Interestingly, the grain stacks parallel many of the microshears identified within this unit. [Colour online.]

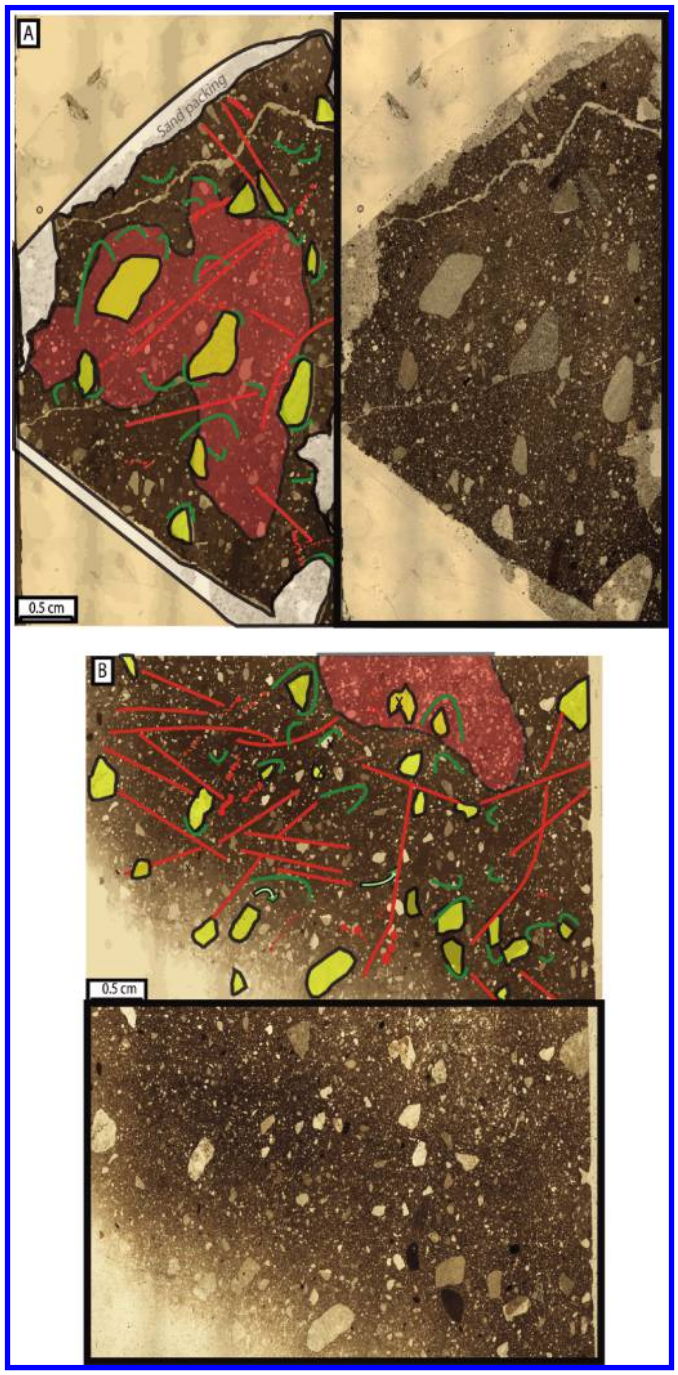

shear angle abundance at the top of Unit C as it transitions to Unit D. Sample PTA-038 illustrates this reduction in low-angle shear structures, followed by an abrupt increase in high-angle shears transitioning into Unit D. The lack of low-angle microshears (<25°) observed in the transition from Unit A to Unit B is tentatively interpreted to reflect the near complete removal of Unit A from the depositional record, as Unit A is only preserved within the bedrock karst depression (Fig. 3). The decrease in low-angle microshears at or just below the contacts of each unit boundary is thought to be the result of a similar process, whereby, low-angled microshears have been destroyed or deformed due to re-mobilization of the upper portions of the unit by the overlying till unit.

Important information is also derived from microstructures identified throughout the thin sections. The presence of shear bands indicates a decrease in effective normal stress, or an increase in shear stress associated with changing subglacial conditions in transition zones at the ephemeral subglacial interface boundary due to changes in basal ice strain, subjacent deforming sediment rheology, and (or) fluctuating basal temperatures (Truffer et al. 2000; van der Meer et al. 2003; Larsen et al. 2007; Phillips et al. 2008; Boulton 2010). Additionally, evidence of pipe-like porewater flow through till sample PTA-030 may indicate pressurized porewater that acted as a conduit to drain water from the till matrix (Phillips and Merritt 2008; Ravier et al. 2014*a*, 2014*b*;

Fig. 14. Annotated thin sections from the uppermost sample collected within Unit C: PTA-038. This sample was packed in sand to prevent disturbance during transport (fine-grained material around sample). Rotation structures, grain stacks, and microshears can be observed. There is a large domain of less clay-rich matrix (highlighted in red), which indicates incomplete homogenization of the unit. [Colour online.]

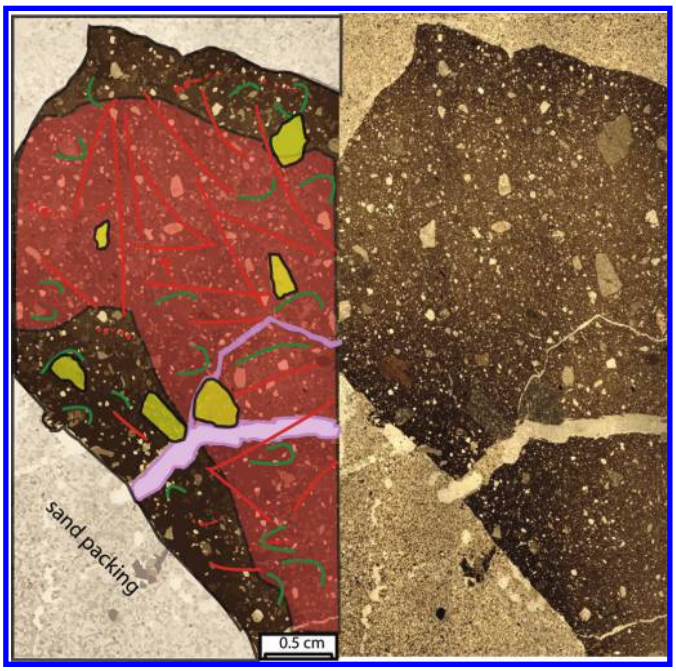

Lelandais et al. 2016). This porewater drainage could have resulted from an increase in the stress on the underlying sediment, which caused localized brecciation, evidence for which can be seen in the large number of voids observed directly below the porewater flow structure (Fig. 11B) (cf. Menzies 1989). Interestingly, sample PTA-030 also has many low-angle shears, suggesting higher levels of stress during deformation. There was a distinct increase in till fissility above this sample that made collecting oriented samples logistically impossible. The significance of this increase remains enigmatic, and further investigation is required, possibly necessitating in situ resin impregnation of the till for sample collection (cf. Lee and Kemp 1992; Carr and Lee 1998; van der Meer and Menzies 2006).

All the thin sections have multiple domains indicative of continuous mixing of at least two till sublithofacies-units throughout till emplacement. In most of the samples, rotation structures are confined to separate domains and that ductile deformation occurred during internal till deformation. Specifically, in Unit C, the number of rotation structures, the lack of edge-to-edge crushing, and tight clustering of shearing angles all indicate higher stress levels, which suggest that this till was deposited by faster-flowing ice (cf. Reinardy et al. 2011; Menzies et al. 2013, 2016*b*). Clast macrofabrics within this unit had the tightest clustering of all measured clast fabrics (Fig. 6) and were oriented along a similar azimuth (Table 3) as the elongated surface landforms in the region (Fig. 2). This implies that Unit C was influenced by relatively fast-flowing ice at some time during its emplacement (cf. McMartin and Paulen 2009).

Shear stress fluctuations during till deformation align well with the evolution path of strain theory outlined by Menzies et al. (2016*a*), whereby fluctuations of shear stress rates have created a set of microstructures as each new till sub-unit is emplaced atop each preceding subjacent immobilized unit. These microstructure assemblages show a temporal sequence of changes in stress

Fig. 15. Annotated thin sections from Unit D: (A) PTA-037 and (B) PTA-040. Rotation structures, microshears, and crushed grains can be observed in both samples. Multiple domains are also evident in the lower of the two samples (PTA-037), indicating an incomplete homogenization of the till unit. The uppermost of these two samples (PTA-040) has an abundance of voids but shows no signs of post-depositional disruption (cf. van Vliet and Langhor 1983). [Colour online.]

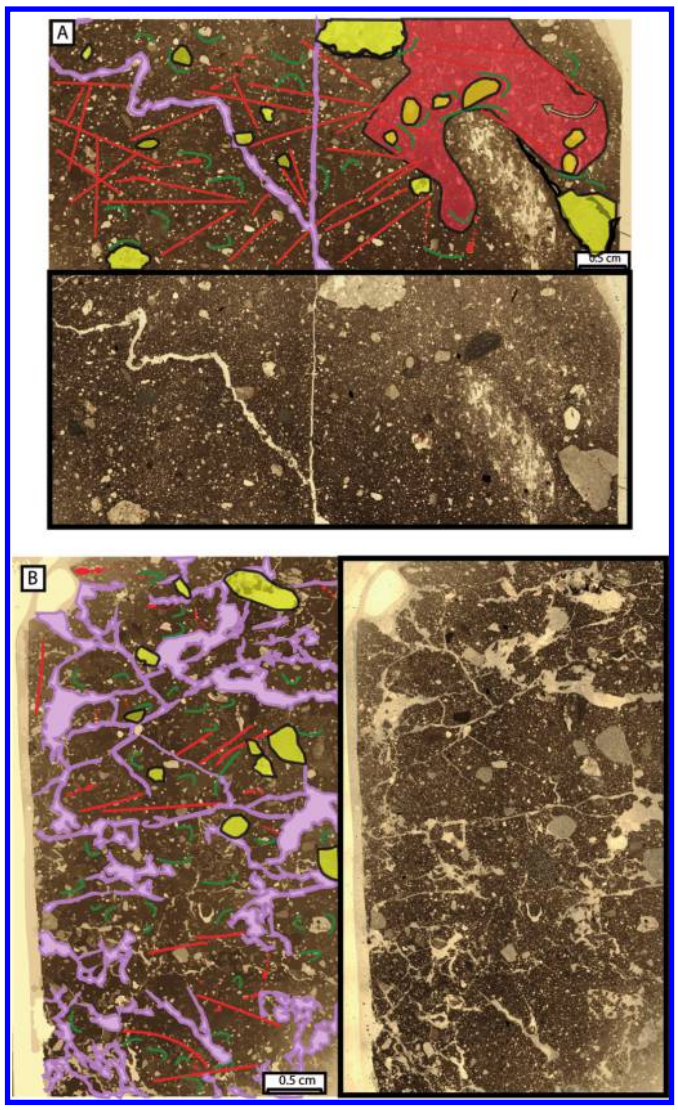

throughout sediment deposition within each till unit. As the overlying ice-mass adjusts to external stress influences, till properties change (new immobilized till sub-units are formed), and stress levels in the upper portion of the deposited till will have many of its stress indicators (i.e., shear lineations) destroyed or altered, as this portion of the till sub-unit deforms as it becomes part of the next subglacial deforming layer (McClenaghan and Paulen 2017). As the deformational interface propagates towards the surface, a contact surface develops between the immobile and mobile layer causing increased stress that creates dilation hardening of the sediment and immobilizes the unit interface (Iverson et al. 1998). In this study, the contact surface is recorded, for example, by a contact between Unit B and Unit C (Fig. 5) whereby the mobile layer is activated and deactivated multiple times, which caused unhomogenized mixing of the units (Menzies 2012). The contact between Unit C and Unit D records the remobilization of Unit C into a viscous layer (Unit D pre-deposition), where large boulders

Fig. 16. Stratigraphic section showing the four till units (separated by dashed lines) and micromorphological sample locations. The angle of measured microshears is plotted on an enclosed bi-directional rose diagram with red bars, indicating shearing angles of low shear strain (<25°) and black bars being angles of high stress levels (>25°). The scatterplot graph indicates relative percentages of high stress angles measured; dashed lines indicate zero data between samples. [Colour online.]

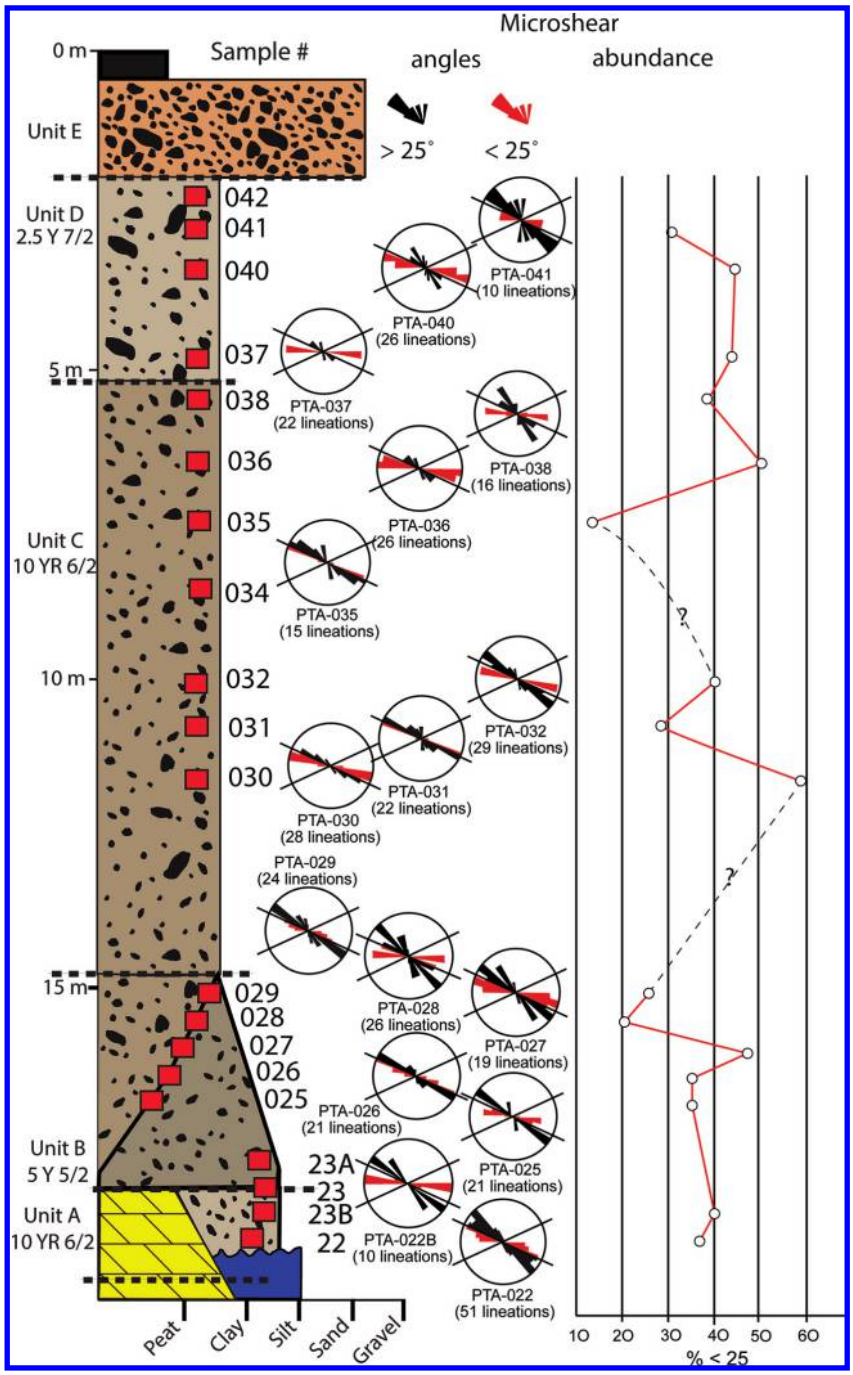

were deformed to the base and deposited as a boulder horizon (Hicock 1991).

This type of mobilization then immobilization between till units has been observed in other deforming till units (Larsen et al. 2006*b*; van der Meer and Menzies 2011; Menzies et al. 2016*b*). These observations fit well within Stanley (2009)'s quantitative aggradational-constant entrainment decay model whereby till layers entrain material from the subjacent till as it moves down-ice, representing continued deformation and mixing of till at the mobile–immobile boundary. DiLabio (1990) suggested that multiple cycles of entrainment caused dispersal trains to rise progressively down-ice. Stanley (2009) proposed that constant entrainment and aggradation of subglacial till caused the features reported by DiLabio (1990) by upward shear imbrication within accumulating till as glaciers flow (cf. Boulton 2006, fig. 2.9). These outcomes correlate well with microshear investigation from subglacial till beneath ice streams that indicate subglacial shearing occurring during till accretion at the top of the deforming bed (Phillips et al. 2018). Our micromorphological observations support the aggradation-constant entrainment decay model, and in addition, also may explain the discontinuities between till layers to be the result of a décollement between the mobile and immobile layer, as evident through

the abundances of low-angle microshear structures measured throughout the till facies.

Conclusions

Micro- and macrosedimentological analyses have been correlated with previously reported geomorphological and sedimentological results (Rice et al. 2013, 2014). From this correlated analysis, subglacial fluctuating rheological conditions have been identified from within specific lithofacies of till units at open-pit K-62 that developed as deforming beds which became immobile and, at times, decoupled from the ice sheet (cf. Boulton and Hindmarsh 1987). Analysis of high-angle microshear abundances in till samples shows evidence of changing till rheology on the sub-unit scale in response to stress fluctuations. These variations are modelled here, either the result of stress intensity that changed prior to aggradation of overlying till sub-units or, more likely, the deformation and (or) obliteration of low-angle shears in underlying units caused by the re-mobilization of the till unit as the overlying immobile sub-unit is subsequently deformed. Due to the spacing of the samples collected and being collected from a single lithofacies, the robustness of the data are limited to these preliminary conclusions. With an increased sample density, higher resolution microshear diagrams could be produced, which would help elucidate what causes the changes between till units and their relations to subglacial stresses. Future work should focus on detailed samples traverse across multiple lithofacies of subglacially deposited till at tighter sample spacing in conjunction with traditional sedimentological analyses. This will allow for a better understanding of the role that the mobile layer plays in stress fluctuations within and between till units.

Acknowledgements

This research was funded by the GSC's Geo-Mapping for Energy and Minerals (GEM) Program (2008–2013) under the Tri-Territorial Indicator Mineral Project and a Research Affiliate Bursary to the senior author. This activity was a contribution to J.M. Rice's M.Sc. thesis at Brock University. The authors thank Stanley Clemmer (Pine Point Mining Limited) for recent access to their exploration diamond drill core that intersected the lowermost till unit (drillhole EX17-DBL-003). Natasha Oviatt (University of Alberta) and Carl Ozyer (Northwest Territories Geological Survey) are thanked for their assistance in the field. We extend our thanks to Martin Ouellette at Brock University for his skilful preparation of thin sections. Rod Smith (Geological Survey of Canada) is thanked for his thorough reviews of an earlier version of this manuscript. The authors also thank Olav Lian and Emrys Phillips for their detailed and thoughtful reviews of this manuscript. NRCan Contribution number/Numéro de contribution de RNCan: 20160177.

References

Banham, P.H. 1988. Polyphase glaciotectonic deformation in the Contorted Drift of Norfolk. *In* Glaciotectonics: Forms and Processes. *Edited by* D.G. Croot. A. A. Balkema, Rotterdam. pp. 27–32.

Benn, D.I. 1994*a*. Fluted moraine formation and till genesis below a temperate valley glacier: Slettmarkbreen, Jotunheimen, southern Norway. Sedimentology, **41**: 279–292. doi:10.1111/j.1365-3091.1994.tb01406.x.

Benn, D.I. 1994*b*. Fabric shape and the interpretation of sediment fabric data. Journal of Sedimentary Research A, **64**: 910–915. doi:10.1306/D4267F05-2B26-11D7-8648000102C1865D.

Benn, D.I. 2004. Chapter 5: Macrofabric. *In* A Practical Guide to the study of glacial sediments. *Edited by* D.J.A. Evan and D.I. Benn. Hodder Education, London, pp. 93–114.

Benn, D.I., and Evans, D.J.A. 1998. Glaciers and Glaciation. Arnold, London.

Boulton, G.S. 2006. Glaciers and their coupling with hydraulic and sedimentary processes. *In* Glacier science and environmental change. *Edited by* P.G. Knight. Wiley-Blackwell, pp. 2–22. doi:10.1002/9780470750636.ch2.

Boulton, G.S. 2010. Drainage pathways beneath ice sheets and their implications for ice sheet form and flow: the example of the British Ice Sheet during the last glacial maximum. Journal of Quaternary Science, **25**: 483–500. doi:10.1002/jqs.1407.

Boulton, G.S., and Hindmarsh, R.C.A. 1987. Sediment deformation beneath glaciers: rheology and geological consequences. Journal of Geophysical Research, **92**: 9059–9082. doi:10.1029/JB092iB09p09059.

Carr, S.J. 1998. The last glaciation of the North Sea Basin. PhD Thesis, Royal Holloway, University of London: 363 p.

Carr, S.J. 1999. The micromorphology of last glacial maximum sediments in the southern North Sea. Catena, **35**: 123–145. doi:10.1016/S0341-8162(98)00097-6.

Carr, S.J. 2001. Micromorphological criteria for distinguishing subglacial and glaciomarine sediments: evidence from a counterparty tidewater glacier, Spitsergen. Quaternary International, **25**: 720–738. doi:10.1016/S1040-6182(01)00051-9.

Carr, S.J. 2004. Micro-scale features and structures. *In* A practical guide to the study of glacial sediments. *Edited by* D.J. Evans and D.I. Benn. Arnold, London, pp. 115–144.

Carr, S.J., and Lee, J.A. 1998. Thin-section production of diamict: problems and solutions. Journal of Sedimentary Research, Section A: Sedimentary Petrology and Processes, **68**: 217–220. doi:10.2110/jsr.68.217.

Carr, S.J., and Rose, J. 2003. Till fabric patterns and significance: particle response to subglacial stress. Quaternary Science Reviews, **22**: 1415–1426. doi:10.1016/S0277-3791(03)00125-2.

Carr, S.J., Hafidason, H., and Sejrup, H.P. 2000. Micromorphological evidence supporting Late Weichselian glaciation of the northern North Sea. Boreas, **29**: 315–328. doi:10.1111/j.1502-3885.2000.tb01213.x.

Chandler, D.M., and Hubbard, B. 2008. Quantifying sample bias in clast fabric measurements. Sedimentology, **55**: 925–938. doi:10.1111/j.1365-3091.2007.00928.x.

Denis, M., Guiraud, M., Konaté, M., and Buoncristiani, J.-F. 2010. Subglacial deformation and water-pressure cycles as a key for understanding ice stream dynamics: evidence from the Late Ordovician succession of the Djado Basin (Niger). International Journal of Earth Sciences, **99**: 1399–1425. doi:10.1007/s00531-009-0455-z.

Dilabio, R.N.W. 1990. Glacial dispersal trains. *In* Glacial Indicator Tracing. *Edited by* R. Kujansuu and M.A.A. Saamisto. Balkema, Rotterdam, pp. 109–122.

Dyke, A.S., Andrews, J.T., Clark, P.U., England, J.H., Miller, G.H., Shaw, J., and Veillette, J.J. 2002. The Laurentide and Innuitian ice sheets during the Last Glacial Maximum. Quaternary Science Reviews, **21**: 9–31. doi:10.1016/S0277-3791(01)00095-6.

Evans, D.J.A. 2018. Till: A Glacial Process Sedimentology. John Wiley and Sons Ltd, London, UK.

Evans, D.J.A., Phillips, E.R., Hiemstra, J.F., and Auton, C.A. 2006. Subglacial till: Formation, sedimentary characteristics and classification. Earth-Science Reviews, **78**: 115–176. doi:10.1016/j.earscirev.2006.04.001.

Eyles, N., Eyles, C., Menzies, J., and Boyce, J. 2011. End moraine construction by incremental till deposition below the Laurentide Ice Sheet: Southern Ontario, Canada. Boreas, **40**: 92–104. doi:10.1111/j.1502-3885.2010.00171.x.

Fossen, H., Soliva, R., Ballas, G., Trzaskos, B., Cavalcante, C., and Schultz, R.A. 2017. A review of deformation bands in reservoir sandstones: geometries, mechanisms and distribution. Geological Society, London, Special Publications, **459**: 1–25. doi:10.1144/SP459.4.

Fossen, H., Cavalcante, G.C.G., Pinheiro, R.V.L., and Archanjo, C.J. 2018. Deformation–Progressive or multiphase? Journal of Structural Geology. In press. doi:10.1016/j.jsg.2018.05.006.

Fulton, R.J. 1995. Surficial materials of Canada. Geological Survey of Canada, "A" Series Map no. 1880A. 1: 5 000 000 scale. doi:10.4095/205040.

Gao, C., McAndrews, J.H., Wang, X., Menzies, J., Turton, C.L., Wood, B.D., et al. 2012. Glaciation of North America in the James Bay Lowland, Canada, 3.5 Ma. Geology, **40**: 975–978. doi:10.1130/G33092.1.

Girrard, I., Klassen, R.A., and Laframboise, R. 2004. Sedimentology laboratory manual, Terrain Sciences Division. Geological Survey of Canada, Open File 4823. doi:10.4095/216141.

Hannigan, R. 2007. Metallogeny of the Pine Point Mississippi Valley-Type lead-zinc district, southern Northwest Territories. *In* Mineral Deposits of Canada: A synthesis of major deposit- types, district metallogeny, the evolution of geological provinces, and exploration methods. *Edited by* W.D. Goodfellow. Geological Association of Canada, Mineral Deposits Division: Special Publication, **5**: 609–632.

Hart, J.K., Hindmarsh, R.C.A., and Boulton, G.S. 1990. Styles of subglacial glaciotectonic deformation within the context of the Anglian ice-sheet. Earth Surface Processes and Landforms, **15**: 227–241. doi:10.1002/esp.3290150305.

Hart, J.K., Rose, K.C., Martinez, K., and Ong, R. 2009. Subglacial clast behaviour and its implication for till fabric development: new results derived from wireless subglacial probe experiments. Quaternary Science Reviews, **28**: 597–607. doi:10.1016/j.quascirev.2008.07.020.

Hicock, S.R. 1991. On Subglacial Stone pavements in till. The Journal of Geology, **99**: 607–619. doi:10.1086/629520.

Hicock, S.R., Goff, J.R., Lian, O.B., and Little, E.C. 1996. On the interpretation of subglacial till fabric. Journal of Sedimentary Research, **6**: 928–934. doi:10.1306/D4268441-2B26-11D7-8648000102C1865D.

Hiemstra, J.F., and van der Meer, J.J.M. 1997. Pore-water controlled grain fracturing as an indicator for subglacial shearing in tills. Journal of Glaciology, **34**: 446–454. doi:10.3189/S0022143000035036.

Hills, E.S. 2012. Elements of structural geology. Springer Science and Business Media, Springer, London, UK.

Hodder, T.J., Ross, M., and Menzies, J. 2016. Sedimentary record of ice divide

migration and ice streams in the Keewatin core region of the Laurentide Ice Sheet. Sedimentary Geology, **338**: 97–114. doi:10.1016/j.sedgeo.2016.01.001.

Hooyer, T.S., and Iverson, N.R. 2000. Clast-fabric development in a shearing granular material: implications for subglacial till and fault gouge. Geological Society of America Bulletin, **112**: 683–692. doi:10.1130/0016-7606(2000)112<683:CDIASG>2.0.CO;2.

Iverson, N.R. 2010. Shear resistance and continuity of subglacial till: hydrology rules. Journal of Glaciology, **56**: 1104–1114. doi:10.3189/002214311796406220.

Iverson, N.R., Hooyer, T.S., and Baker, R.W. 1998. Ring-shear studies of till deformation: Coulomb-plastic behavior and distributed strain in glacier beds. Journal of Glaciology, **44**: 634–642. doi:10.3189/S0022143000002136.

Jørgensen, F., and Piotrowski, J.A. 2003. Signature of the Baltic Ice Stream on Funen Island, Denmark during the Weichselian glaciation. Boreas, **32**: 242–255. doi:10.1111/j.1502-3885.2003.tb01440.x.

Kleman, J., and Glasser, N.F. 2007. The subglacial thermal organization (STO) of ice sheets. Quaternary Science Reviews, **26**: 585–597. doi:10.1016/j.quascirev.2006.12.010.

Lachniet, M.S., Larson, G.J., Lawson, D.E., Evenson, E.B., and Alley, R.B. 2001. Microstructures of sediment flow deposits and subglacial sediments: a comparison. Boreas, **30**: 254–262. doi:10.1111/j.1502-3885.2001.tb01226.x.

Larsen, N.K., Piotrowski, J.A., and Kronborg, C. 2004. A multiproxy study of a basal till: a time-transgressive accretion and deformation hypothesis. Journal of Quaternary Science, **19**: 9–21. doi:10.1002/jqs.817.

Larsen, N.K., Piotrowski, J.A., and Christiansen, F. 2006*a*. Microstructures and microshears as proxy for strain in subglacial diamicts: implications for basal till formation. Geology, **34**: 889–892. doi:10.1130/G22629.1.

Larsen, N.K., Piotrowski, J.A., Christoffersen, P., and Menzies, J. 2006*b*. Formation and deformation of basal till during a glacier surge: Elisebreen, Svalbard. Geomorphology, **81**: 217–234. doi:10.1016/j.geomorph.2006.04.018.

Larsen, N.K., Piotrowski, J.A., and Menzies, J. 2007. Microstructural evidence of low-strain, time-transgressive subglacial deformation. Journal of Quaternary Science, **22**: 593–608. doi:10.1002/jqs.1085.

Lee, J., and Kemp, R. 1992. Thin sections of unconsolidated sediments and soils: a recipe. Centre for Environmental Analysis and Management (CEAM), Royal Holloway, University of London, CEAM Technical Report, **2**: 1–32.

Lee, J.R., and Phillips, E.R. 2008. Progressive soft sediment deformation within a subglacial shear zone – a hybrid mosaic – pervasive deformation model for Middle Pleistocene glaciotectonised sediments from eastern England. Quaternary Science Reviews, **27**: 1350–1362. doi:10.1016/j.quascirev.2008.03.009.

Lelandais, T., Mourgues, R., Ravier, É., Pochat, S., Strzerzynski, P., and Bourgeois, O. 2016. Experimental modeling of pressurized subglacial water flow: Implications for tunnel valley formation. Journal of Geophysical Research- Earth Surface, **121**: 2022–2041. doi:10.1002/2016JF003957.

Lemmen, D.S. 1990. Surficial material associated with glacial Lake McConnell, southern District of Mackenzie. *In* Current Research, Part D. Geological Survey of Canada Paper, **90–1d**: 79–83. doi:10.4095/131342.

Lemmen, D.S. 1998*a*. Surficial geology, Klewi River, District of Mackenzie; Northwest Territories. Geological Survey of Canada, "A" Series Map 1905, scale 1:250 000. doi:10.4095/209686.

Lemmen, D.S. 1998*b*. Surficial geology, Buffalo Lake, District of Mackenzie; Northwest Territories. Geological Survey of Canada, "A" Series map 1906, scale 1:250 000. doi:10.4095/209687.

Lemmen, D.S., Duk-Rodkin, A., and Bednarski, J.M. 1994. Late glacial drainage systems along the northwestern margin of the Laurentide Ice Sheet. Quaternary Science Reviews, **13**: 805–822. doi:10.1016/0277-3791(94)90003-5.

Licht, K.J., Dunbar, N.W., Andrews, J.T., and Jennings, A.E. 1999. Distinguishing subglacial till and glacial marine diamicton in the western Ross Sea, Antarctica: Implications for a last glacial maximum grounding line. Geological Society of America Bulletin, **111**: 91–103. doi:10.1130/0016-7606(1999)111<0091:DSTAGM>2.3.CO;2.

Maltman, A.J. 1988. The importance of shear zones in naturally deformed wet sediments. Tectonophysics, **145**: 163–175. doi:10.1016/0040-1951(88)90324-1.

Margold, M., Stokes, C.R., and Clark, C.D. 2015. Ice streams in the Laurentide Ice Sheet: identification, characteristics and comparison to modern ice sheets. Earth-Science Reviews, **143**: 117–146. doi:10.1016/j.earscirev.2015.01.011.

Marshall, S.J., and Clark, P.U. 2002. Basal temperature evolution of North American ice sheets and implications for the 100-kyr cycle. Geophysical Research Letters, **29**: 671–674. doi:10.1029/2002GL015192.

McClenaghan, M.B., and Paulen, R.C. 2017. Chapter 20: Application of till mineralogy and Geochemistry to Mineral exploration. *In* Past Glacial Environments (second edition). *Edited by* J. Menzies and J.J.M. van der Meer. Elsevier, pp. 689–751. doi:10.1029/2002GL015192.

McClenaghan, M.B., Oviatt, N.M., Averill, S.A., Paulen, R.C., Gleeson, S.A., McNeil, R.J., et al. 2012. Indicator mineral abundance data for bedrock, till and stream sediment samples from the Pine Point Mississippi Valley-Type Zn-Pb deposits, Northwest Territories. Geological Survey of Canada, Open File 7267. doi:10.4095/292121.

McMartin, I., and Henderson, P.J. 2004. Evidence from Keewatin (Central Nunavut) for Paleo-Ice Divide Migration. Géographie Physique et Quaternaire, **58**: 163–186. doi:10.7202/013137ar.

McMartin, I., and Paulen, R. 2009. Ice-flow indicators and the importance of ice-flow mapping for drift prospecting. *In* Application of Till and Stream Sediment Heavy Mineral and Geochemical Methods to Mineral Exploration in Western and Northern Canada. *Edited by* R.C. Paulen and I. McMartin. Geological Association of Canada. Short Course Notes, **18**: 15–34. doi:10.7202/013137ar.

Menzies, J. 1989. Subglacial hydraulic conditions and their possible impact upon subglacial bed formation. Sedimentary Geology, **62**: 125–150. doi:10.1016/0037-0738(89)90112-7.

Menzies, J. 2000. Micromorphological analyses of microfabrics and microstructures indicative of deformation processes in glacial sediments. *In* Deformation of glacial materials. *Edited by* B. Hubbard and M.J. Hambrey. London Maltman, Geological Society Special Publication No. 176. London: pp. 245–257. doi:10.1144/GSL.SP.2000.176.01.19.

Menzies, J. 2012. Strain pathways, till internal architecture and microstructures-perspectives on a general kinematic model- a 'blueprint' for till development. Quaternary Science Reviews, **50**: 105–124. doi:10.1016/j.quascirev.2012.07.012.

Menzies, J., and Ellwanger, D. 2011. Insights into subglacial processes inferred from the micromorphological analyses of complex diamicton stratigraphy near Illmensee-Lichtenegg, Höchsten, Germany. Boreas, **40**: 271–288. doi:10.1111/j.1502-3885.2010.00194.x.

Menzies, J., and Maltman, A.J. 1992. Microstructures in diamictons - evidence of subglacial bed conditions. Geomorphology, **6**: 27–40. doi:10.1016/0169-555X(92)90045-P.

Menzies, J., and van der Meer, J.J.M. 2018. Micromorphology and microsedimentology of glacial sediments. *In:* Past Glacial Environments (Second Edition). *Edited by* J. Menzies and J.J.M. van der Meer. Elsevier, pp. 753–806. doi:10.1016/B978-0-08-100524-8.00036-1.

Menzies, J., and Reitner, J.M. 2016. Microsedimentology of ice-stream tills from the eastern Alps, Austria — a new perspective on till microstructures. Boreas, **45**: 804–827. doi:10.1111/bor.12189.

Menzies, J., and Whiteman, C. 2009. A comparative analysis of microstructures from Late Jurassic diamictic units, near Helmsdale, northeast Scotland and a Pleistocene diamicton from near Milton, southern Ontario, Canada — a differential diagnostic method of sediment typing using micromorphology. Netherlands Journal of Geosciences, **88**: 75–94. doi:10.1017/S0016774600001001.

Menzies, J., and Zaniewski, K. 2003. Microstructures within a modern debris flow deposit derived from Quaternary glacial diamicton – a comparative micromorphological study. Sedimentary Geology, **157**: 31–48. doi:10.1016/S0037-0738(02)00193-8.

Menzies, J., van der Meer, J.J.M., and Rose, J. 2006. Till—as a glacial "tectomict", its internal architecture, and the development of a "typing" method for till differentiation. Geomorphology, **75**: 172–200. doi:10.1016/j.geomorph.2004.02.017.

Menzies, J., Gao, C., and Kodors, C. 2013. Microstructural analyses of a Middle Pliocene till from the James Bay Lowlands, Canada—evidence of "potential" fast ice streaming. Proceedings of the Geologists' Association, **124**: 790–801. doi:10.1016/j.pgeola.2012.07.002.

Menzies, J., van der Meer, J.J.M., and Ravier, E. 2016*a*. A kinematic unifying theory of microstructures in subglacial tills. Sedimentary Geology, **344**: 57–70. doi:10.1016/j.sedgeo.2016.03.024.

Menzies, J., Hess, D.P., Rice, J.M., Wagner, KG., and Ravier, E. 2016*b*. A case study in the New York drumlin field, an investigation using microsedimentology, resulting in the refinement of a theory of drumlin formation. Sedimentary Geology, **338**: 84–96. doi:10.1016/j.sedgeo.2016.01.017.

Menzies, J., van der Meer, J.J.M., and Shilts, W.W. 2018. Chapter 5: Subglacial Processes and Sediment. *In* Past Glacial Environments (Second Edition). *Edited by* J. Menzies and J.J.M. van der Meer. Elsevier, pp. 105–158.

Morgenstern, N.R., and Tchalenko, J.S. 1967. Microscopic structures in kaolin subjected to direct shear. Géotechnique, **17**: 309–328. doi:10.1680/geot.1967.17.4.309.

Murphy, C.P. 1986. Thin section preparation of soils and sediments. AB Academic Publication, Berkhamsted.

Narloch, W., Piotrowski, J.A., Wysota, W., Larsen, N.K., and Menzies, J. 2012. The signature of strain magnitude in tills associated with the Vistula Ice Stream of the Scandinavian Ice Sheet, central Poland. Quaternary Science Reviews, **57**: 105–120. doi:10.1016/j.quascirev.2012.09.022.

Neudorf, C.M., Brennand, T.A., and Lian, O.B. 2013. Till-forming processes beneath parts of the Cordilleran Ice Sheet, British Columbia, Canada: macroscale and microscale evidence and a new statistical technique for analyzing microstructures data. Boreas, **42**: 848–875. doi:10.1111/bor.12009.

Neudorf, C.M., Brennand, T.A., and Lian, O.B. 2015. Comparison between macro- and microfabrics in a pebble-rich, sandy till deposited by the Cordilleran Ice Sheet. Boreas, **44**: 438–501. doi:10.1111/bor.12120.

Oviatt, N.M., and Paulen, R.C. 2013. Surficial geology, Breynat Point, NTS 85-B/15, Northwest Territories. Geological Survey of Canada. Canadian Geoscience Map 114, scale 1:50 000. doi:10.4095/293452.

Oviatt, N.M., McClenaghan, M.B., Paulen, R.C., Gleeson, S.A., Averill, S.A., and Paradis, S. 2013*a*. Indicator minerals in till and bedrock samples from the Pine Point Mississippi Valley-type district, Northwest Territories. Geological Survey of Canada Open File 7423. doi:10.4095/293031.

Oviatt, N.M., McClenaghan, M.B., Paulen, R.C., and Gleeson, S.A. 2013*b*. Till geochemical signatures of the Pine Point Pb-Zn Mississippi Valley-type district, Northwest Territories. Geological Survey of Canada Open File 7320. doi:10.4095/292906.

Oviatt, N.M., Gleeson, S.A., Paulen, R.C., McClenaghan, M.B., and Paradis, S. 2015. Characterization and dispersal of indicator minerals associated with the Pine Point Mississippi Valley-Type (MVT) District, Northwest Territories, Canada. Canadian Journal of Earth Sciences, **52**: 776–794. doi:10.1139/cjes-2014-0108.

Passchier, C.W., and Trouw, R.A.J. 1996. Micro-tectonics. Springer Verlag, Berlin-Heidelberg, Germany.

Phillips, E. 2006. Micromorphology of a debris flow deposit: evidence of basal shearing, hydrofracturing, liquefaction and rotational deformation during emplacement. Quaternary Science Reviews, **25**: 720–738. doi:10.1016/j.quascirev.2005.07.004.

Phillips, E., and Auton, C.A. 2000. Micromorphological evidence for polyphase deformation of glaciolacustrine sediments from Strathspey, Scotland. *In* Deformation of glacial materials. *Edited by* A.J. Maltman, B. Hubbard, and H.J. Hambrey. Geological Society London, Special Publications, **176**: 279–292. doi:10.1144/GSL.SP.2000.176.01.21.

Phillips, E., and Lee, J.R. 2013. Development of a subglacial drainage system and its effect on glacitectonism within the polydeformed Middle Pleistocene (Anglian) glacigenic sequence of north Norfolk, Eastern England. Proceedings of the Geologists' Association, **124**: 855–875. doi:10.1016/j.pgeola.2012.07.005.

Phillips, E., and Merritt, J. 2008. Evidence for multiphase water-escape during rafting of shelly marine sediments at Clava, Inverness-Shire, NE Scotland. Quaternary Science Reviews, **27**: 988–1011. doi:10.1016/j.quascirev.2008.01.012.

Phillips, E., Merritt, J., Auton, C., and Golledge, N.R. 2007. Microstructures in subglacial and proglacial sediments: understanding faults, folds and fabrics, and the influence of water on the style of deformation. Quaternary Science Reviews, **26**: 1499–1528. doi:10.1016/j.quascirev.2007.03.007.

Phillips, E., Lee, J.R., and Burke, H. 2008. Progressive proglacial to subglacial deformation and syntectonic sedimentation at the margins of the Mid-Pleistocene British Ice Sheet: evidence from north Norfolk, UK. Quaternary Science Reviews, **27**: 1848–1871. doi:10.1016/j.quascirev.2008.06.011.

Phillips, E., van der Meer, J.J.M., and Ferguson, A. 2011. A new 'microstructural mapping' methodology for the identification, analysis and interpretation of polyphase deformation within subglacial sediments. Quaternary Science Reviews, **30**: 2570–2596. doi:10.1016/j.quascirev.2011.04.024.

Phillips, E., Everest, J., and Reeves, H. 2013. Micromorphological evidence for subglacial multiphase sedimentation and deformation during overpressurized fluid flow associated with hydrofracturing. Boreas, **42**: 395–427. doi:10.1111/j.1502-3885.2012.00261.x.

Phillips, E., Spagnolo, M., Pilmer, A.C.J., Rea, B.R., Piotrowski, J.A., Ely, J.C., and Carr, S. 2018. Progressive ductile shearing during till accretion within the deforming bed of a palaeo-ice stream. Quaternary Science Reviews, **193**: 1–23. doi:10.1016/j.quascirev.2018.06.009.

Piotrowski, J.A., Larsen, N.K., Menzies, J., and Wysota, W. 2006. Formation of subglacial till under transient bed conditions: deposition, deformation, and basal decoupling under a Weichselian Ice Sheet Lobe, central Poland. Sedimentology, **53**: 83–106. doi:10.1111/j.1365-3091.2005.00755.x.

Plouffe, A., McClenaghan, M.B., Paulen, R.C., McMartin, I., Campbell, J.E., and Spirito, W.A. 2013. Processing of glacial sediments for the recovery of indicator minerals: protocols used at the Geological Survey of Canada. Geochemistry: Exploration, Environment, Analysis, **13**: 303–316. doi:10.1144/geochem2011-109.

Prest, V.K., Grant, D.R., and Rampton, V.N. 1968. Glacial map of Canada. Geological Survey of Canada, Map 1253A, scale 1:5 000 000. doi:10.4095/108979.

Ravier, E., Buoncristiani, J.-F., Guiraud, M., Menzies, J., Clerc, S., Goupy, B., and Portier, E. 2014*a*. Porewater pressure control on subglacial soft sediment remobilization and tunnel valley formation: A case study from the Alnif tunnel valley (Morocco). Sedimentary Geology, **304**: 71–95. doi:10.1016/j.sedgeo.2014.02.005.

Ravier, E., Buoncristiani, J.-F., Clerc, S., Guiraud, M., Menzies, J., and Portier, E. 2014*b*. Sedimentological and deformational criteria for discriminating subglaciofluvial deposits from subaqueous ice-contact fan deposits: A Pleistocene example (Ireland). Sedimentology, **61**: 1382–1410. doi:10.1111/sed.12111.

Reinardy, B.T.I., Hiemstra, J.F., Murray, T., Hillenbrand, C.D., and Larter, R.D. 2011. Till genesis at the bed of an Antarctic peninsula palaeo-ice stream as indicated by micromorphological analysis. Boreas, **40**: 498–517. doi:10.1111/j.1502-3885.2010.00199.x.

Rice, J.M., Paulen, R.C., Menzies, J., McClenaghan, M.B., and Oviatt, N.M. 2013. Glacial stratigraphy of the Pine Point Pb-Zn Mine Site, Northwest Territories. Geological Survey of Canada, Current Research, **2013-5**: 1–14. doi:10.4095/292184.

Rice, J.M., Paulen, R.C., Menzies, J., and McClenaghan, M.B. 2014. Micromorphological descriptions of till from pit K-62, Pine Point Mining District, Northwest Territories. Geological Survey of Canada Open File 7526. doi:10.4095/293478.

Ringrose, T.J., and Benn, D.I. 1997. Confidence regions for fabric shape diagrams. Journal of Structural Geology, **19**: 1527–1536. doi:10.1016/S0191-8141(97)00077-1.

Roberts, D.H., and Hart, J.K. 2005. The deforming bed characteristics of a stratified till assemblage in north East Anglia, UK: investigating controls on sediment rheology and strain signatures. Quaternary Science Reviews, **24**: 123–140. doi:10.1016/j.quascirev.2004.03.004.

Shilts, W.W., and Kettles, I.M. 1990. Geochemical-mineralogical profiles through fresh and weathered till. *In* Glacier indicator tracing. *Edited by* R. Kujansuu and M. Saarnisto. Balkema, Rotterdam, pp. 187–216.

Skall, H. 1975. The paleoenvironment of the Pine Point lead-zinc district. Economic Geology, **70**: 22–47. doi:10.2113/gsecongeo.70.1.22.

Skolasińska, K., Rachlewicz, G., and Szczuciński, W. 2016. Micromorphology of modern tills in southwestern Spitsbergen – Insights into depositional and post-depositional processes. Polish Polar Research, **37**: 435–456. doi:10.1515/popore-2016-0023.

Smith, D.G. 1994. Glacial Lake McConnell: paleogeography, age, duration and associated ricer deltas, Mackenzie River basin, western Canada. Quaternary Science Reviews, **13**: 829–843. doi:10.1016/0277-3791(94)90004-3.

Spagnolo, M., Phillips, E., Piotrowski, J.A., Rea, B.R., Clark, C.D., Stokes, C.R., et al. 2016. Ice stream motion facilitated by a shallow-deforming and accreting bed. Nature Communications, **7**: 1–11. doi:10.1038/ncomms10723.

Stanley, C.R. 2009. Geochemical, mineralogical and lithological dispersal models in glacial till: physical processes constraints and application. *In* mineral exploration in Application of Till and Stream Sediment Heavy Mineral and Geochemical Methods to Mineral Exploration in Western and Northern Canada. *Edited by* R.C. Paulen and I. McMartin. GAC Short Course Notes, **18**: 35–48.

Stokes, C.R., Tarasov, L., and Dyke, A.S. 2012. Dynamics of the North American Ice Sheet Complex during its inception and build-up to the Last Glacial Maximum. Quaternary Science Reviews, **50**: 86–104. doi:10.1016/j.quascirev.2012.07.009.

Tarasov, L., and Peltier, W.R. 2007. Coevolution of continental ice cover and permafrost extent over the last glacial-interglacial cycle in North America. Journal of Geophysical Research: Earth Science, **112**: 1–13. doi:10.1016/j.quascirev.2012.07.009.

Tchalenko, J.S. 1968. The evolution of kink-bands and the development of compression textures in sheared clays. Tectonophysics, **6**: 159–174. doi:10.1016/0040-1951(68)90017-6.

Tchalenko, J.S. 1970. Similarities between shear zones of different magnitudes. Geological Society of America Bulletin, **81**: 1625–1640. doi:10.1130/0016-7606(1970)81[1625:SBSZOD]2.0.CO;2.

Tembe, S., Lockner, D.A., and Wong, T.-F. 2010. Effect of clay content and mineralogy on frictional sliding behavior of simulated gouges: binary and ternary mixtures of quartz, illite, and montmorillonite. Journal of Geophysical Research, **115**: B03416. doi:10.1029/2009JB006383.

Thomason, J.F., and Iverson, N.R. 2006. Microfabric and microshear evolution in deformed till. Quaternary Science Reviews, **25**: 1027–1038. doi:10.1016/j.quascirev.2005.09.006.

Trommelen, M.S., Ross, M., and Campbell, J.E. 2013. Inherited clast dispersal patterns: Implications for palaeoglaciology of the SE Keewatin Sector of the Laurentide Ice Sheet. Boreas, **42**: 693–713. doi:10.1111/j.1502-3885.2012.00308.x.

Truffer, M., Harrison, W.D., and Echelmeyer, K.A. 2000. Glacier motion dominated by processes deep in underlying till. Journal of Glaciology, **46**: 213–221. doi:10.3189/172756500781832909.

van der Meer, J.J.M. 1993. Microscopic evidence of subglacial deformation. Quaternary Science Reviews, **12**: 553–587. doi:10.1016/0277-3791(93)90069-X.

van der Meer, J.J.M. 1997. Particle and aggregate mobility in till: microscopic evidence of subglacial processes. Quaternary Science Reviews, **16**: 827–831. doi:10.1016/S0277-3791(97)00052-8.

van der Meer, J.J.M., and Menzies, J. 2006. Handbook Sixth International Workshop on the Micromorphology of Glacial Sediments. Department of Geosciences, Hamilton College, NY.

van der Meer, J.J.M., and Menzies, J. 2011. The micromorphology of unconsolidated sediments. Sedimentary Geology, **238**: 213–232. doi:10.1016/j.sedgeo.2011.04.013.

van der Meer, J.J.M., Menzies, J., and Rose, J. 2003. Subglacial till: the deforming glacier bed. Quaternary Science Reviews, **22**: 1659–1685. doi:10.1016/S0277-3791(03)00141-0.

van Vliet, B., and Langhor, R. 1983. Evidence of disturbance by frost of pore ferri-argillans in silty soils of Belgium and northern France. *In* Soil Micromorphology. *Edited by* P. Bullock and C.P. Murphy. AB Academic Press, University of Michigan, pp. 511–518.

Vaughan-Hirsch, D.P., Phillips, E., Lee, J.R., and Hart, J.K. 2013. Micromorphological analysis of poly-phase deformation associated with the transport and emplacement of glaciotectonic rafts at West Runton, North Norfolk, UK. Boreas, **42**: 376–394. doi:10.1111/j.1502-3885.2012.00268.x.

Winsborrow, M.C.M., Clark, C.D., and Stokes, C.R. 2004. Ice streams of the Laurentide Ice Sheet. Géographie Physique et Quaternaire, **58**: 269–280. doi:10.7202/013142ar.

Wolfe, S.A., Huntley, D.J., and Ollerhead, J. 2004. Relict Late Wisconsinan dune fields of the northern Great Plains, Canada. Géographie physique et Quaternaire, **58**: 323–336. doi:10.7202/013146ar.